MATHEMATICAL MODELING OF BIOCHEMICAL INFLUENCES AND LIVE CELL IMAGING OF BIOPHYSICAL INFLUENCES ON ADIPOSE-DERIVED MESENCHYMAL STEM CELL BEHAVIOR

by

Hetty Nie

A thesis submitted to the Faculty of the University of Delaware in partial fulfillment of the requirements for the Degree of Master of Science in Biomedical Engineering

Spring 2017

MATHEMATICAL MODELING OF BIOCHEMICAL INFLUENCES AND LIVE CELL IMAGING OF BIOPHYSICAL INFLUENCES ON ADIPOSE-DERIVED MESENCHYMAL STEM CELL BEHAVIOR

by

Hetty Nie

Approved: _____
John H. Slater, Ph.D.
Professor in charge of thesis on behalf of the Advisory Committee

Approved: _____
Thomas Buchanan, Ph.D.
Chair of the Department of Biomedical Engineering

Approved: _____
Babatunde Ogunnaike, Ph.D.
Dean of the College of Engineering

Approved: _____
Ann L. Ardis, Ph.D.
Senior Vice Provost for Graduate and Professional Education

ACKNOWLEDGMENTS

I would like to express my gratitude to my advisor, Dr. John Slater, for his guidance and support during my graduate school career. Similarly, I would like to extend appreciation to my lab mates and fellow biomedical graduate students for not only their scientific insight, but also their comradery. Without them and their suggestions, not only would research have been more difficult, but life would have been less colorful.

I would like to acknowledge Dr. Jeffry Caplan and Michael Moore at the Delaware Biotechnology Institute's Bioimaging Center for their invaluable knowledge and assistance in operating the confocal microscopes.

I would like to acknowledge Dr. Dawn Elliott and Dr. John Peloquin for the use and training in use of their Instron compression testing machine, and, similarly, Alexander Mitkas and Janty Shoga for their Matlab expertise.

I would like to acknowledge the friends I have made through the Graduate Student Government and, in particular, Janice Hudson for their unwavering support, new perspectives of data, without whom this thesis would not have been possible.

Lastly, I would like to thank non-affiliated friends and family for their encouragement.

TABLE OF CONTENTS

Chapter

LIST OF TABLES

LIST OF FIGURES

ABSTRACT

Stem cell therapy holds promise in treating and curing diseases that currently do not have efficacious treatment options. However, the most efficient method of differentiating stem cells is unknown. Here, we present two novel approaches to capture temporal behavior of stem cells. First, we quantify biochemical influences by developing a mathematical model that captures the differentiation behavior of stem cells over the course of two weeks and describes differentiation behavior using rate constants. Our cell differentiation is congruent with the media formulation (e.g. statistically significant osteogenesis occurs in osteogenic media and statistically significant adipogenesis occurs in adipogenic media). We use two modeling methods, maximum likelihood and least squares to extrapolate differentiation rate constants. We disprove the equal rates hypothesis for differentiation rates and show that the presence of one differentiation marker influences the ability of cells to develop a contrasting differentiation marker. While the differentiation rates do not clearly describe trends between differentiation in varying media, comparing the ratio of the rates show the dynamics. By looking at the ratio of rates we are able to describe which phenotype will dominate by describing how quickly each population of stem cells positive for one marker becomes positive for both. This model provides a basis to compare differentiation as a function of different biochemical and biophysical cues in terms of rate constants. Next, we characterize biophysical influences of ASC behavior, particularly adhesion site dynamics, using hydrogel substrates with stiffness values congruent with bone and fat. We show that while the number of adhesions between cells on different substrates are not statistically significant, the size of adhesions developed on soft and stiff substrates are. We prove our hypothesis that stem cells on

x

stiff substrates develop large, stable adhesions that their counterparts on soft substrates cannot. This implies that cells on stiff substrates may be able to bear greater forces across adhesions and activate signaling pathways that cannot be activated on soft substrates.

Chapter 1

INTRODUCTION

1.1   Stem Cells

Stem cells are defined by two properties, potency and self-renewal[1]. Potency describes the innate ability of stem cells to differentiate into a terminal cell line. Potency varies depending on the origin of the stem cell from monopotent, the ability to differentiate only into one terminal cell line, to totipotent the ability to differentiate into any cell line in the body given the appropriate stimuli. Self-renewal describes the stem cell's ability to continuously generate more stem cells.

Embryonic stem cells are totipotent but are met with a slew of ethical issues hindering their clinical use. Therefore, adult stem cells have become the preferred source of stem cells for investigation[2]. The next stage when embryos develop is to have three germ layers, the endoderm, the mesoderm, and the ectoderm. The endoderm develops into the digestive tract; the mesoderm develops into the musculoskeletal system and internal organs; the ectoderm develops into the integumentary system.

For target tissues, such as muscle and bone, that are largely derived from the mesoderm, the stem cells of interest are mesenchymal stem cells[3]. Mesenchymal stem

cells are a multipotent stem cell, meaning that they are capable of committing to several, but not all adult lineages. Mesenchymal stem cells have successfully been differentiated down osteogenic (bone)[4], adipogenic (fat)[5], chondrogenic (cartilage)[6], neurogenic (nerve)[7], and myogenic (muscle)[6] lineages.

Bone marrow-derived mesenchymal stem cells have historically been used most frequently due to an interest into differentiating stem cells into bone[8]. Recently, adipose-derived stem cells have also been successfully differentiated down osteogenic lineages[9]. This discovery has increased the popularity of adipose tissue as an alternative source of adult mesenchymal stem cells because of the higher density of stem cells in the tissue and also the relative ease of tissue acquisition compared to bone marrow[9].

1.2   Stem Cell Therapies

Because of pluripotency and self-renewal, stem cell-based therapies hold great promise in treating a myriad of diseases that currently have sub optimal or no treatment options[1]. Many degenerative diseases from neurological[10], to muscular[11], to osteoporosis[12] fall into this category. The ultimate goal of stem cell therapy is to allow medical practitioners to isolate stem cells from individual patients, terminally differentiate the stem cells into the necessary adult lineage, and re-implant a functional tissue. By using patient derived cells, adverse immune responses can be avoided, and may stimulate the patient's tissue to maintain healthy function.

Additionally, stem cells are an attractive source for the development of microtissues for uses in high throughput drug screening. Stem cells may be able to be differentiated into a variety of representative microtissue (e.g. lungs, gut, kidney, etc.) that will accurately represent an individual's response to treatment. This idea of microtissues or "human on a chip[13]" can potentially revolutionize the concept of personalized medicine. This approach could be particularly attractive for use in screening treatments for genetic disease or diseases such as cancer that vary widely from person to person causing generic treatment to have a huge variety in terms of efficacy.

1.3   Stem Cell Niches

Toward the development of previously described therapeutics and screening devices, many current approaches use naïve stem cell[14]. However, efficacy of stem cell therapies may be increased by priming cells toward a lineage of interest. Classically, stem cell differentiation is induced by chemical growth factors. However, recent advances show physical factors are able to induce stem cell differentiation independently of chemical growth factors[4,15]. The distinct combinations of lineage specific biochemical and biophysical factors compose a stem cell niche[16]. Stem cell lineage commitment may be induced by any number of environmental factors that are representative of a stem cell niche. For example: substrate stiffness modulation induces differentiation of stem cells. Soft environments around 1 kPa lead to increased

3

adipogenesis while those around .1 kPa favor neurogenesis, medium stiffness (10 kPa) induces myogenesis and stiffer environments (40 kPa) are more likely to induce osteogenesis[17,18]. Although stiffness dependent differentiation has been established, it is not without complications. In many studies that were conducted, decreasing the stiffness of the material also resulted in an increased porosity of the material.[19] Additionally, the substrate thickness plays a role in the ability of cells to sense their environment. Substrates that are too thin will not replicate representative behavior as the glass or silicon the soft gel is mounted on interferes with the propagation of stresses and strains. This resulting in cells sensing an effective stiffness that is stiffer than the substrate[20,21].

Cellular tension also plays an important role in differentiating stem cells. Micropatterns can be used to modulate cell shape or spreading, and therefore, cell tension by limiting the adhesive area available to cells[22]. By creating cell adhesive micropatterns surrounded by non-adhesive materials, cells will adopt the desired shape. Manipulating micropattern parameters such as area[15], aspect ratio[4], and curvature[4], result in different cell behaviors. Higher percentages of cells on micropatterns that were large, had high aspect ratios, and low curvature underwent osteogenesis compared to their counterparts on small, low aspect ratios, and high curvature that favored adipogenesis[4,14].

Additionally, extracellular matrix composition may influence the differentiation of cells independently of the substrate stiffness. Since different extracellular matrix proteins present different integrin binding sites, the recruitment of

distinct integrins or combinations of integrins will initiate different downstream signaling cascades that affect gene expression and result in vastly different phenotypes. For example, the peptide sequence arginine-glycine-aspartic acid-serine (RGDS) is derived from fibronectin and interacts with $\alpha_v\beta_3$ integrins[23] which is not known to influence stem cell differentiation. However, fibronectin proteins also recruit $\alpha_5\beta_1$ integrins that are upregulated during osteogenic priming of adipose derived stem cells[24]. Therefore the use of peptide sequences may not recapitulate the same behavior as whole proteins, but conversely, allow for engineered control over integrin recruitment.

The exact mechanism of mechanotransduction remains poorly characterized. While the YAP/TAZ pathway assists cells in mechanical sensing[25] and plays a role in cell fate determination[26], it is not a comprehensive explanation. Current hypothesis suggests that vinculin, a mechanosensitive adhesion site protein, undergoes a conformational change under actin mediated stress[27]. The conformational change reveals a cryptic binding site for MAPK, a protein essential to a plethora of high-impact signaling pathways including, but not limited to proliferation, migration, and stem cell differentiation[27,28].

How multiple methods of mechanical sensing interact remains largely unknown. Similarly, the effect of each component in a stem cell niche or the interplay of how they bolster or contradict lineage commitment is ambiguous. It is difficult to determine the individual effects of biophysical and biochemical signals, and furthermore, biophysical factors are difficult to decouple. Ultimately, it is unclear how

to combine these factors to create an efficient, high-yielding stem cell differentiation environment.

1.4   Heterogeneity within Stem Cell Populations

Unfortunately, experiments performed using adult stem cells are often confounded by heterogeneity in the starting stem cell population. Even within populations that appear isogenic, subpopulation effects still confound whole-population trends, and interesting or useful subpopulation effects can be obscured by whole-population quantification methods[29].

Heterogeneity within stem cells arises from many different potential sources. First, tissues from which the cells are harvested contain undifferentiated, partially differentiated, and fully differentiated cells. The separation of undifferentiated cells may not be complete before use in experiments. Second, stem cells harvested even from a single tissue may already be primed toward different lineages which changes their potency and may cause the cells to be likely to differentiate down different lineages even when exposed to the same stimuli[29]. Another source of heterogeneity is that commercially available sources are often pooled, meaning that even a single vial will contain cells from multiple donors and contain additional confounding factors.

To reduce the influences of population heterogeneity, single cell quantification techniques are increasing in popularity and availability. However, it is difficult to temporally measure single cells. Most established quantification methods require cell

fixation resulting in only one temporal measurement[30]. Therefore to investigate

temporal effects, each time point must be collected from a different sub population,

allowing sub-population effects to add additional variability and, therefore, error to the

analysis.

Alternative approaches center around live cell imaging. While live cell

imaging eliminates variability derived from observing distinct sub-populations, the

imaging process, particularly prolonged exposure to light, can potentially interfere

with cell behavior. Therefore, heterogeneity continues to confound temporal stem cell

analysis and increases error as it interferes with the ability to accurately measure and

isolate whole- and subpopulation trends[30]

1.5   Mathematical Modeling of Stem Cell Differentiation

Mathematical modeling allows us to predict and quantify biological trends and

phenomena. By fitting experimental data to mathematical models, we can better

understand and characterize trends. Additionally, feedback from mathematical models

help design better and more meaningful experiments. However, since mathematical

models require simplification of real-world behavior, every facet of the system may

not be captured. In developing a mathematical model, we isolate the most influential

factors to the system and analyze how those factors are related.

Very few models have been developed previously to describe stem cell lineage

commitment. A recent model has suggested a bi-stable switch where mesenchymal

stem cells have the option of remaining stem cells or making a mutually exclusive, non-reversible decision to become either myogenic or osteogenic[31]. However, this model does not fully describe differentiation behavior, neglecting cell populations that present multiple markers.

While mathematical models tend to simplify certain aspects of biology, having a mathematical model of stem cell behavior begins to create a standard for comparing the influences of different differentiation factors. Currently, it is difficult to compare and optimize biochemical and biophysical factors that influence the differentiation of stem cells, but using a model to extract information, such as differentiation rate constants, we can create a metric that can be compared across the different differentiation conditions.

1.6   Novelty

Our studies propose two novel ways to examine cell behavior with respect to biochemical and biophysical cues. First, we created a mathematical model that captured the differentiation behavior of adipose derived mesenchymal stem cells. We use model simulations and experimental data to quantify the behavior of stem cells subjected to different media compositions. Our modeling simulations reveal that it is not necessarily the differentiation rate, but the ratio of rates that describe the differentiation behavior. By comparing the rate of developing the first differentiation marker to that of the second differentiation marker, we are able to describe the differentiation into both phenotypes and whether adipogenesis or osteogenesis will

dominate the remaining population. Next, we present a live cell imaging technique using fluorescently labeled talin to track the behavior of stem cells on substrates of different stiffness. The biophysical influences of stiffness are captured in the cell adhesion site behavior. We propose adhesion dynamics as a metric for measuring cell behavior because vinculin, a protein recruited to adhesion sites contains a cryptic MAPK binding site. Adhesion site behavior may reveal downstream temporal signaling based on tension loaded on vinculin

Chapter 2

METHODS & MATERIALS

2.1   Cell Culture

ASC52telo human telomerase reverse transcriptase (hTERT) immortalized adipose derived mesenchymal stem cells were purchased from American Type Culture Collection (ATCC). Cells were cultured in tissue culture flasks in low serum stem cell maintenance media and maintained at 37C and aerated with 95% air and 5% CO_2. Cells were passaged at 70% confluence. Cells were lifted using three minute incubation with 0.25% trypsin. The trypsin was deactivated with trypsin neutralizing solution and centrifuged at 13500 rpm. Cells were seeded at 5000 cells/cm^2 into 24 well plates for differentiation studies and 500 cells/cm^2 for live cell imaging studies. Cells were allowed to adhere overnight and the media was replaced with differentiation media. Osteogenic and pre-adipocyte (adipogenic) singlequots were purchased from Lonza to supplement low glucose, L-Glutamine free, phenol free Dulbecco's Modified Eagle Medium. Mixed media was created by combining a 1:1 ratio of osteogenic and adipogenic media

2.2   Immunohistochemistry

Cells were grown in 24 well plates and fed media every 3 days by replacing half of the media with fresh media. Cells were fixed and stained at 0, 3, 6, 7, 9, 12, 14,

15, 18, 21 days. Cells were rinsed three times with sterile phosphate buffered saline and fixed in 4% paraformaldehyde in phosphate buffered saline for 5 minutes at room temperature. Cells were rinsed three times with sterile phosphate buffered saline.

To stain the cells for osteogenic potential, cells were incubated in a filtered fast blue working solution of 4% napthol as-mx phosphatase (4-Chloro-2methylbenzenediazonium/3-Hydroxy-2-napthoic acide 2, 30dimethylanilide phosphate) in water with 1% fast blue salt for one hour in the dark. Cells were rinsed three times with phosphate buffered saline.

To stain cells for lipid droplet production, cells were first rinsed with 100% isopropyl alcohol and then 60% isopropyl alcohol in water. Cells were incubated with 3% oil red o in 60% isopropyl alcohol for 20 minutes. Cells were then rinsed with 60% isopropyl alcohol and then rinsed three times with non-sterile phosphate buffered saline.

To stain cell nuclei, cells were incubated in 10 µg/ml Hoechst stain in phosphate buffered saline for half an hour. Cells were rinsed three times with non-sterile phosphate buffered saline and then stored in 0.2% sodium azide in non-sterile phosphate buffered saline at 4C.

2.3   Wide Field Image Acquisition and Image Analysis

Wide field images of stem cell differentiation were acquired using an inverted Zeiss Axiovert microscope and a Zeiss color camera. Transmitted images were

acquired using a 100ms exposure time and 2.1 volt lamp intensity. Fluorescent images were acquired using a 500 ms exposure time and 58.3% lamp power under the dapi channel. Image analysis was performed using ImageJ cell counter to identify cell nuclei and evaluate differentiation markers in the corresponding transmitted image.

2.4   Statistical Analysis

Statistical analysis was performed using three-way ANOVA on differentiation between different media types at the one and two week time points. Least Squares regression analysis was performed to determine the most accurate method and assumptions of the mathematical model. Two- and one- way ANOVA was performed on cell adhesion data to determine differences in adhesion number and size, respectively, between cells on soft and stiff substrates.

2.5   Mathematical Modeling

Mathematical modeling was performed using a custom written Matlab code. We developed a series of ordinary differential equations that describe differentiation. Cells are separated into four populations, or modeling compartments, determined by the presence of osteogenic markers (O), adipogenic markers (A), both (B) or neither (N). Cells that were positive for neither were assumed to be stem cells capable of self renewal at a rate of k_1 and differentiate into osteogenic cells (O) at a rate of k_2 and adipogenic cells (A) at a rate of k_4 (eq 1). Osteogenic (O) differentiation from stem

cells (N) can then develop adipogenic markers and become positive for both (B) at a rate of k_5 (eq 2). Similarly, adipogenic (A) differentiation from stem cells (N) can develop osteogenic markers at a rate of k_3 and also become both (B) (eq 3).

$$\frac{dM}{dt} = k_1\, N - k_2\, N - k_4\, N \tag{1}$$

$$\frac{dO}{dt} = k_2\, N - k_5\, O \tag{2}$$

$$\frac{dA}{dt} = k_4 N - k_3\, A \tag{3}$$

$$\frac{dB}{dt} = k_5\, O + k_3\, A \tag{4}$$

Experimental data was imported from excel and compared to a maximum likelihood and least square approximation that then exported estimated rate values.

2.6 Material Characterization

Poly(ethylene glycol) diacrylate (PEGDA) gels were photopolymerized using a UV source and lithium phenyl-2,4,6-trimethylbenzoylphosphinate (LAP) as a photoinitiator. A pre-polymer solution of 10% w/v PEGDA, 1.5 mg/ml LAP in HBS and a polymerization time of 2 minutes was used to achieve a stiff gel (1.16±.12 kPa) and A pre-polymer solution of 7% w/v PEGDA, 1 mg/ml concentration of LAP in

HBS, and a polymerization time of 45 seconds was used to achieve a soft gel (101±23 kPa).

Ligand incorporation was characterized using a fluorescently-tagged, peptide-labeled, monoacrylate PEG molecule. Bulk PEGDA hydrogels were soaked in a solution of the fluorescently-tagged, protein-labeled, monoacrylate PEG for a minimum of one hour and re-exposed to a UV source for 30 seconds to 1 minute. The fluorescent signal of bulk hydrogels was evaluated using fluorescence microscopy.

Gel stiffness was characterized by polymerizing gels with a thickness of 1 mm and compressing to an indentation distance of 0.55 mm using an Instron mechanical tester. Assuming linear elasticity, the compressive modulus and elastic modulus should be equal. Elastic modulus was extrapolated at 15% strain using a custom Matlab code to evaluate force curves at 15% strain. Compression testing was performed on gels prior to- and post- ligand incorporation.

Hydrogels used for cell culture experiments were micromolded against acrylated cover slips and adhered to petri dishes with double-sided sticky tape. The gels were sterilized overnight in 70% ethanol. Sterile gels were placed into a biosafety cabinet and the ethanol rinsed three times for 30 minutes with sterile PBS.

2.7   Live Cell Imaging

Human adipose derived mesenchymal stem cells were grown using the above method. Prior to imaging, cells were transduced with GFP-talin, by adding 50

adenovirus particles per cell to the media, incubated overnight, and rinsed with mixed media the following morning. Successful transduction was confirmed using wide field fluorescence microscopy. Live cell imaging was performed the evening after rinsing using a Zeiss 710 inverted microscope equipped with an incubated stage enclosure at 37C and 5% CO_2. Prior to live cell imaging, cells were exposed to the adenovirus overnight and media changed to remove viruses the following morning. Images were acquired at 30 second intervals for 45 minutes using 1% 488 laser power, scan speed of 5, averaging of 2, and high resolution (1800 x 1500 px) window.

.

Chapter 3

RESULTS

3.1 Stem Cell Differentiation as a Function of Biochemical Influences

Stem cell differentiation is dependent upon soluble factors found in the media. Factors promoting adipogenesis include insulin,insulin like growth factor, macrophage colony stimulating factors, glucocorticoids and many more[32]. Conversely, factors promoting osteogenesis include, but are not limited to bone morephogenic protine, endothelin-1, lipcalin-2, and prolactin[33]. Here, we use osteogenic and adipogenic soluble factors to preferentially drive stem cells toward a given fate. Although stem cell differentiation as a function of soluble factors is well established, we aim to combine temporal experimental data of adipose derived mesenchymal stem cells with a mathematical model that will characterize the behavior using rate constants.

To study the temporal differentiation of stem cells under the influences of different media compositions, we characterized the phenotype of cells at different time points for the presence of alkaline phosphatase activity and lipid droplet formation. Alkaline phosphatase activity is indicated by fast blue staining that is cleaved by alkaline phosphatase, resulting in the inability of fast blue to exit the cell and also a color change. Lipid droplets were identified using an oil red o dye that stains lipids red. (Figure 3.1)
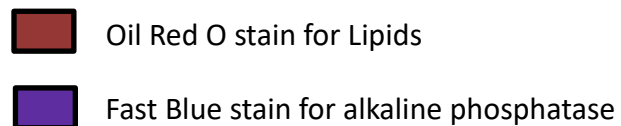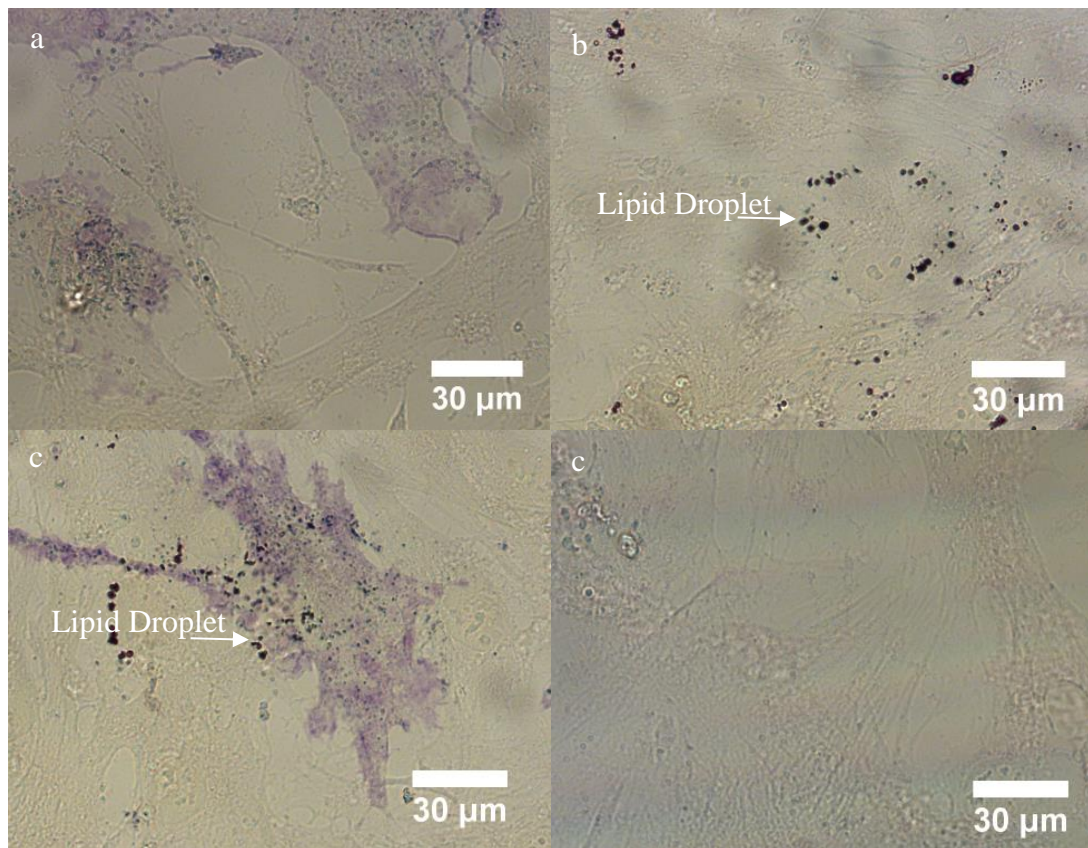
Figure 3.1: Representative Images of Immunohistochemical Staining. Mesenchymal stem cells were stained and quantified using wide field microscopy to gather colored images. Images were analyzed for the presence of osteogenic and adipogenic markers resulting in four distinct populations of cells. Cells with (a) distinctive blue-purple splotches from fast blue staining were characterized as osteogenic while those with (b) red circular lipid bubbles from oil red o staining were characterized as adipogenic. Some cells presented (c) both purple splotches and red circular lipid bubbles or (d) neither of these markers.

We quantified stem cell differentiation every 3 days to capture the temporal aspect of stem cell differentiation and included time points at 7 and 14 days. 7 and 14 days are common time points in literature and were included for potential comparison in the future. However, the 3 day time points allows us to observe stem cell differentiation behavior with a much finer temporal mesh. Initial cell populations were largely negative for both osteogenic and adipogenic markers, but contained a sub population of cells positive for at least one differentiation marker. Osteogenesis and adipogenesis occurred in all three media compositions and resulted in a cell population predominantly positive for both markers. (Fig. 3.2)

In osteogenic media, osteogenesis increased to 4.00% on day 7 and fluctuated until day 14 at 34.1% of the population. Conversely, adipogenesis remained relatively low, never exceeding 11.5%, and cells that presented both markers increased, becoming the dominating population at 54.1%. (Fig. 3.3) In adipogenic media, osteogenesis still fluctuated but remained relatively low never exceeding 12.4%, adipogenesis increased reaching a peak of 43.9% on day 9, and cells presenting both markers increased as well reaching 60.7% on day 14. (Fig. 3.4) In mixed media, osteogenesis remained relatively low peaking at 27.2% on day 6. Adipogenesis increased over the two weeks reaching 23.6% of the population, and cells presenting both markers increased to 63.6% at day 14 and became the majority by day 9. (Fig. 3.5) Differentiation between media compositions displayed similar trends (Fig. 3.6). The differentiation trends are largely congruent with their respective media

composition. However, the high percentage of populations positive for both markers is unexpected and unprecedented.

Additionally, the proliferation data shows different trends between cells in osteogenic and adipogenic media. Both media contain the same percentage of serum which indicates two different possibilities. First, osteogenic pathways could potentially share signaling cascades with proliferation, and soluble factors meant to induce osteogenesis are also inducing proliferation in stem cells. Second, we assume that only stem cells are able to undergo proliferation, and this assumption may not be accurate. Osteogenic cells and adipogenic cells have pre-osteogenic and pre-adipogenic counterparts that have distinct growth rates.

Subsequent statistical analysis revealed that osteogenesis was significantly different ($p<.05$) at day 7 between cells treated with either osteogenic or adipogenic media, and osteogenesis and adipogenesis were significantly different ($p<.05$) at day 14. Differences were also significant ($p<.05$) for osteogenesis between osteogenic and mixed media at 14 days, but differences for other populations between mixed media, osteogenic media, and adipogenic media are largely non-significant. (Table 3.1).
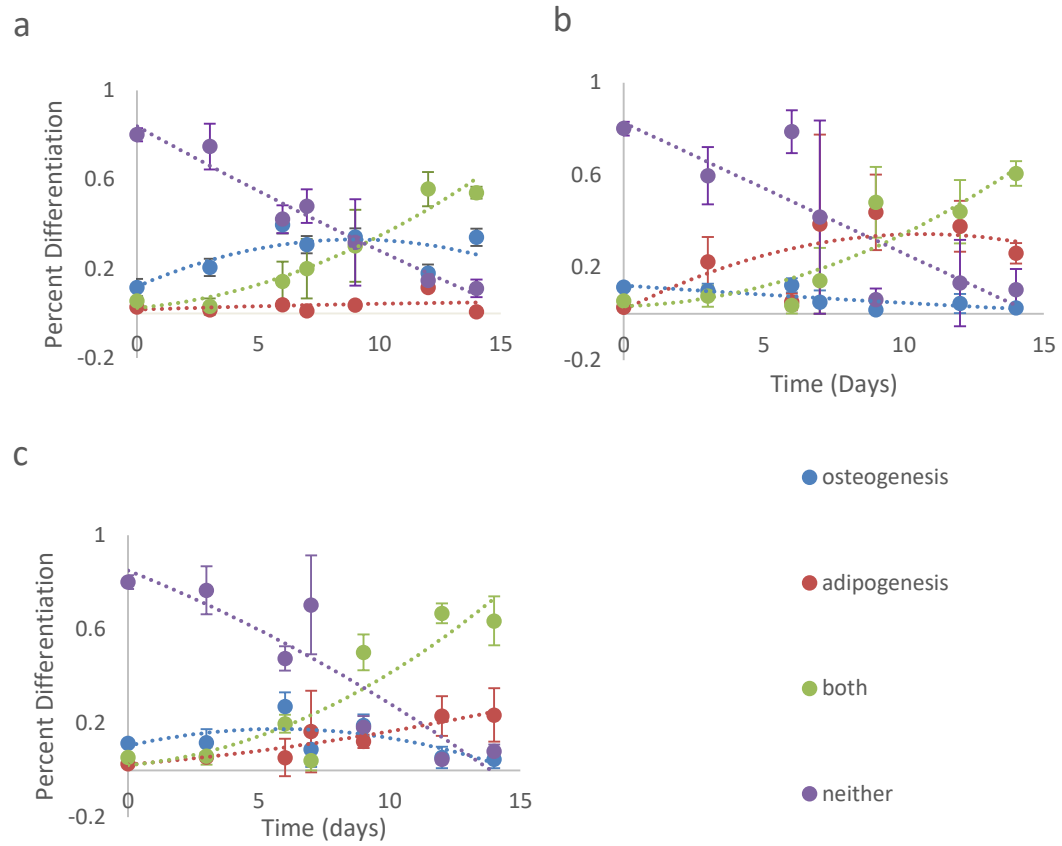
Figure 3.2 Percent Differentiation Over Time as a Function of Media Composition. Mesenchymal stem cells differentiated in (a) osteogenic media, (b) mixed media, and (c) adipogenic media quantified for osteogenic and adipogenic markers.
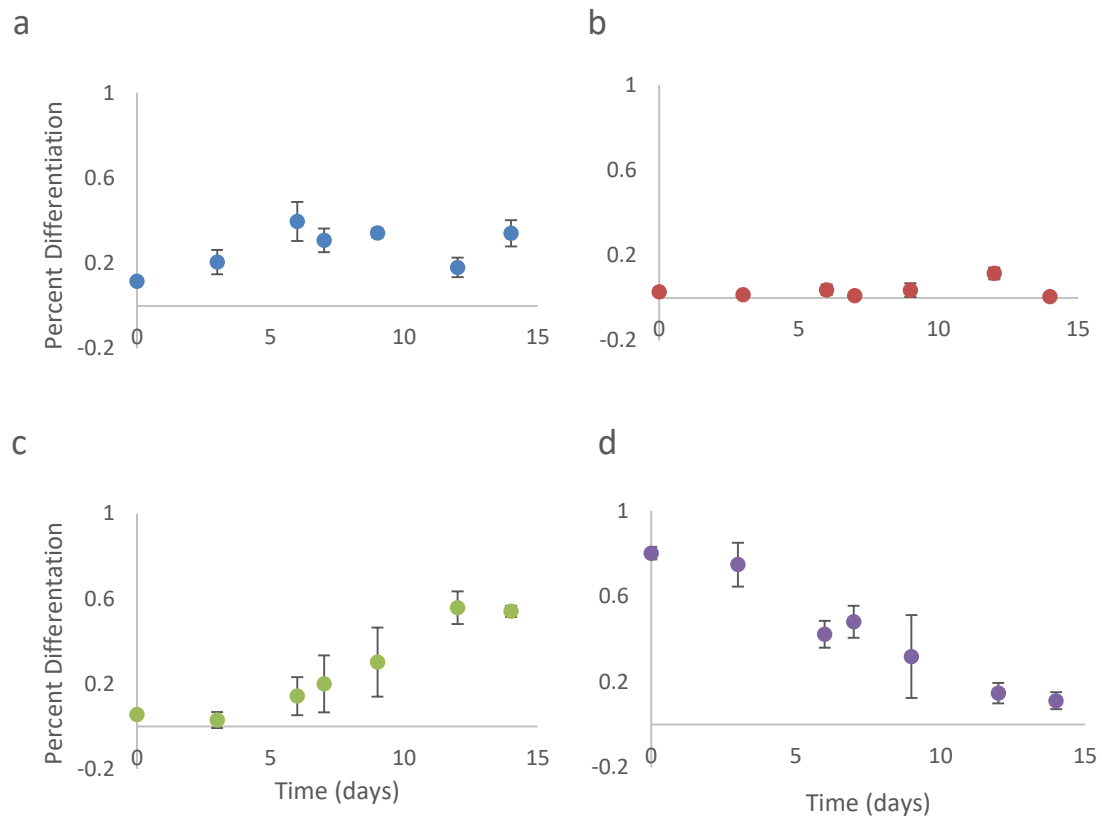
Figure 3.3 Percent Differentiation Over Time in Osteogenic Media Mesenchymal stem cells differentiated in osteogenic media quantified for cells presenting (a) osteogenic, (b) adipogenic, (c) both or (d) neither adipogenic or osteogenic markers.
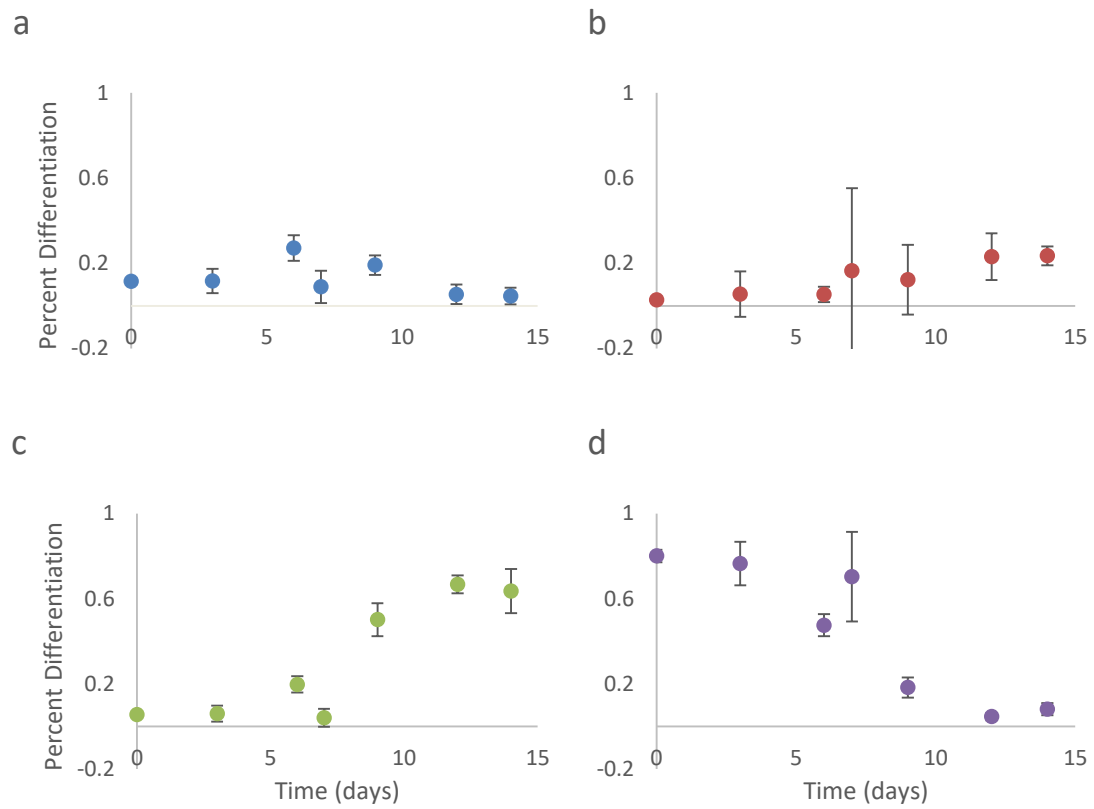
Figure 3.4 Percent Differentiation Over Time in Adipogenic Media. Mesenchymal
stem cells differentiated in adipogenic media quantified for cells
presenting (a) osteogenic, (b) adipogenic, (c) both or (d) neither
adipogenic or osteogenic markers.
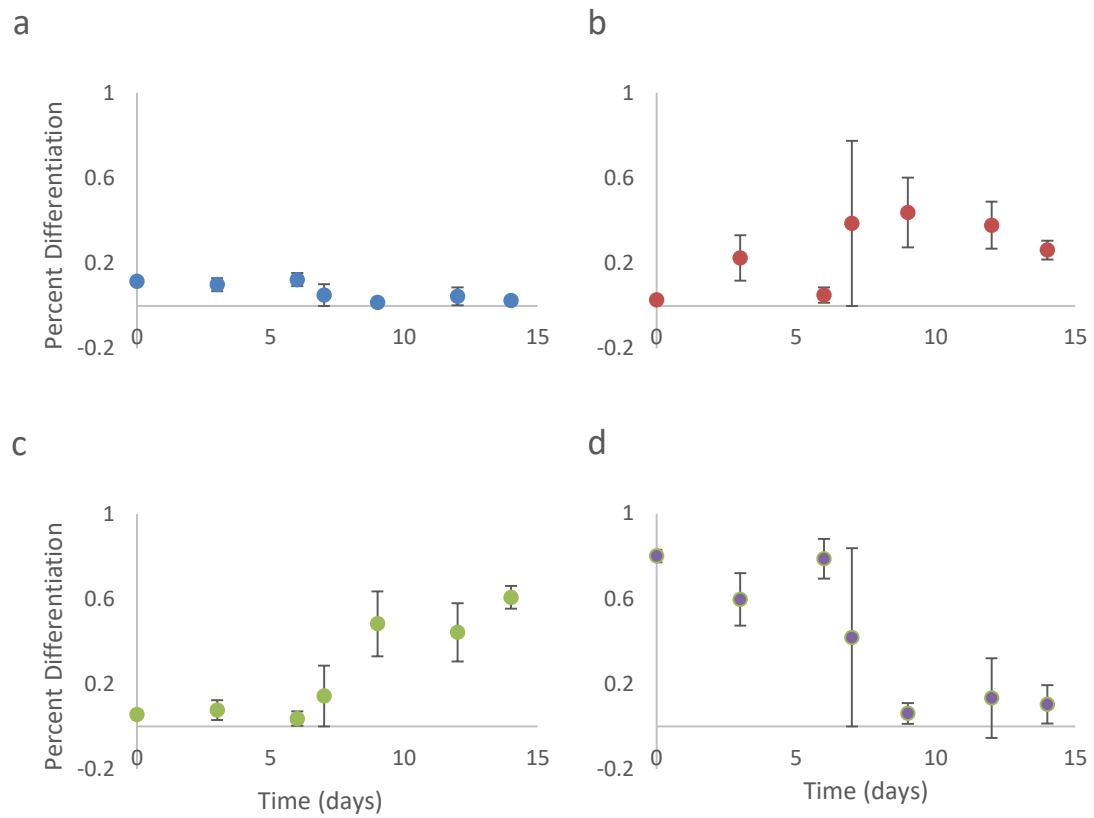
Figure 3.5 Percent Differentiation Over Time in Mixed Media. Mesenchymal stem cells differentiated in mixed media quantified for cells presenting (a) osteogenic, (b) adipogenic, (c) both or (d) neither adipogenic or osteogenic markers.
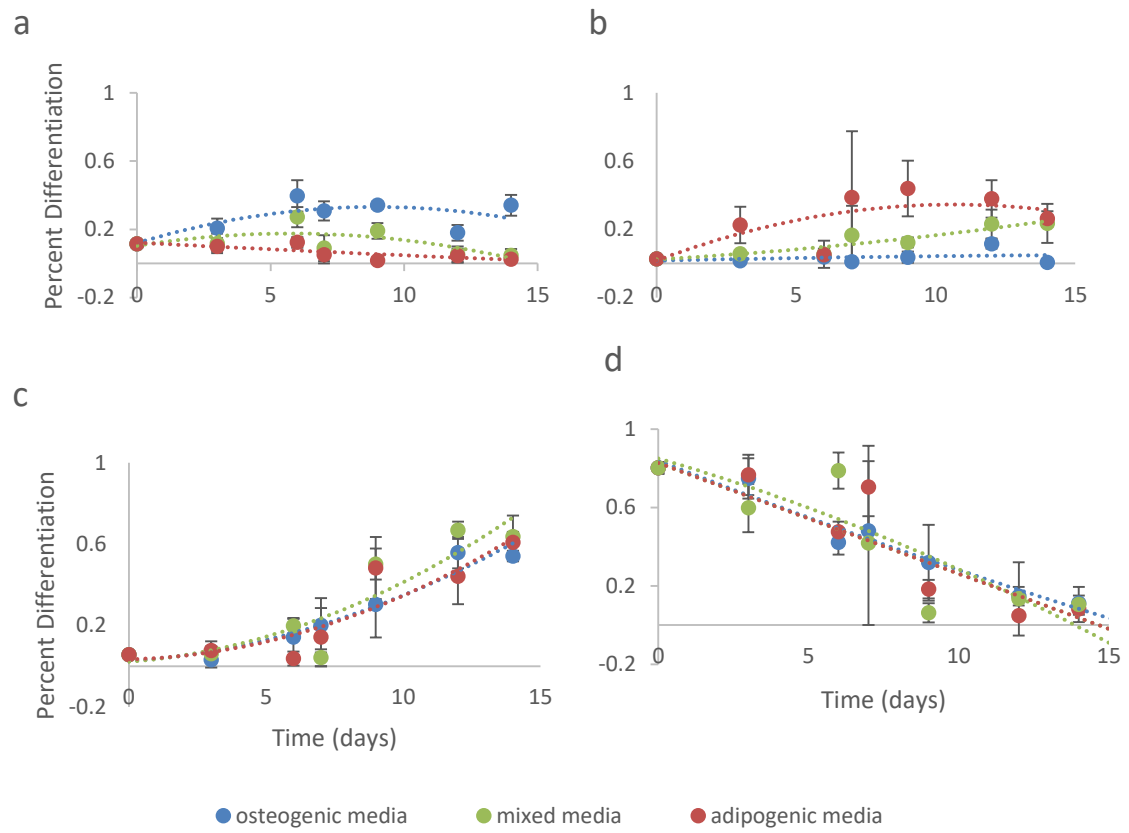
Figure 3.6 Comparisons of Percent Differentiation Over Time across Different Media
Compositions. Mesenchymal stem cells differentiated in osteogenic,
mixed, and adipogenic media quantified for cells presenting (a)
osteogenic, (b) adipogenic, (c) both or (d) neither adipogenic or
osteogenic markers.

Differentiation	Osteogenic	Adipogenic	Both	Neither
Comparison	Osteogenic Media & Mixed Media			
D7	0.103	0.281	0.162	0.144
D14	0.003	0.077	0.334	0.074
Comparison	Adipogenic Media & Mixed Media			
D7	0.718	0.262	0.149	0.130
D14	0.496	0.980	0.302	0.040
Comparison	Osteogenic and Adipogenic Media			
D7	0.006	0.139	0.193	0.618
D14	0.012	0.001	0.425	0.025

Table 3.1 Three-Way ANOVA of Differentiation. Three-way anova p values for differentiation as a function of media. P values <.05 are significant and p values of <.01 are extremely significant.
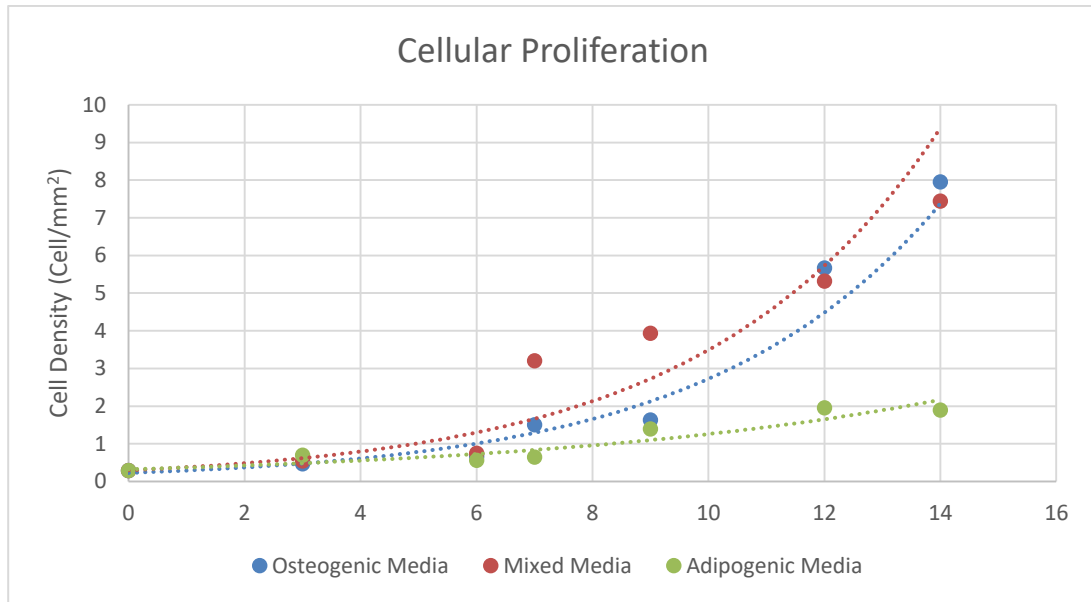
Figure 3.7 Comparisons of Cell Proliferation Over Time across Different Media
    Compositions. Mesenchymal stem cell proliferation in osteogenic media,
    mixed media, and adipogenic media ofer the course of two weeks.

3.2   Mathematical Modeling of Stem Cell Differentiation Behavior

Mathematical modeling helps predict and quantify differentiation behavior. By applying this model to our experimental data, we can quantify and compare the differentiation rates of stem cells subject to different media conditions. Additionally, analysis of these rates begins to elucidate a mathematical description of stem cell behavior. Further, we can apply our model to future differentiation experiments on both biochemical and biophysical cues and use the simulated rate constants to compare the differentiation behavior across these experiments.

Using a series of ordinary differential equations, we describe the differentiation behavior. Cells positive for neither osteogenic nor adipogenic markers were classified as stem cells (N) with the ability to self-renew at a rate of k_1. These stem cells could then differentiate into either osteogenic or adipogenic cells at the rates of k_2 and k_4 respectively. These osteogenic and adipogenic cells present with the contrasting lineage's marker with rates of k_5 and k_3 respectively. (Fig. 3.8)

$$\frac{dM}{dt} = k_1 N - k_2 N - k_4 N$$

$$\frac{dO}{dt} = k_2 N - k_5 O$$

$$\frac{dA}{dt} = k_4 N - k_3 A$$

$$\frac{dB}{dt} = k_5 O + k_3 A$$
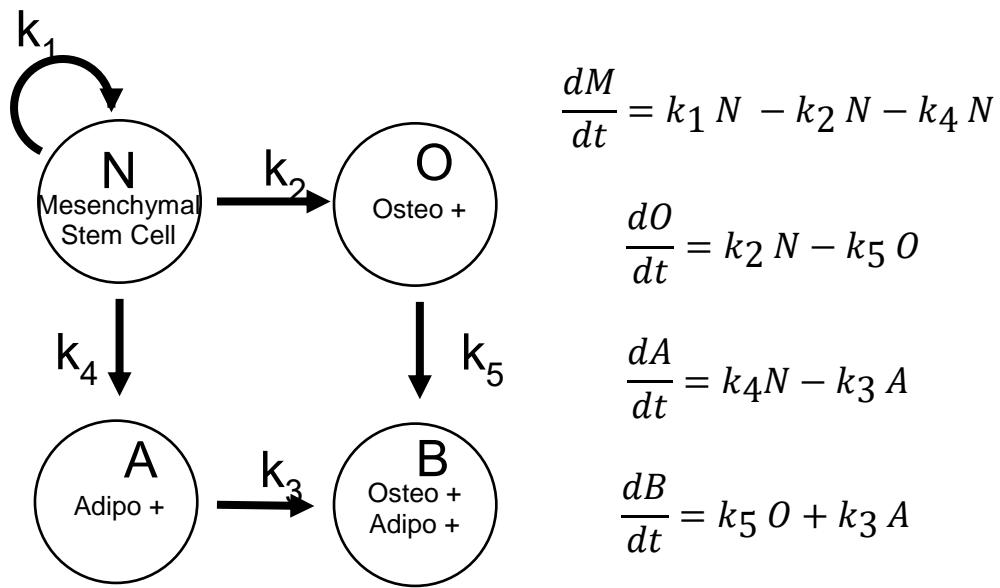
Figure 3.8 Graphical Representation of Mathematical Ordinary Differential Equation Model. Complete model of the compartments of stem cell differentiation and the equations derived ordinary differential equations

To model the data, two different methods are used. The least squares method and the maximum likelihood method. The least squares method optimizes the sum of the squares of the differences between the experimental data and the model to predict the most accurate rate reaction value. The least square approach can be efficiently solved using matrix algebra but fails when the relationship between the variables is not linear[34]. The maximum likelihood estimation assumes the population is normally distributed, and applies a normal distribution to the data to back-calculate the most likely mean and variance for the population. The maximum likelihood method is a versatile estimation useful for large samples and is applicable to most models and many types of data, and in many cases, is able to capture phenomena with greater accuracy and precision. However, the maximum likelihood estimation may be difficult to calculate and solve[34].

Here, we opted to use both models and compare the resulting simulations. To simplify the equations, cell populations were assumed to have logistic growth. Both model simulations were applied to experimental data in osteogenic media (Fig. 3.9), adipogenic media (Fig 3.10), and mixed media (Fig 3.11).
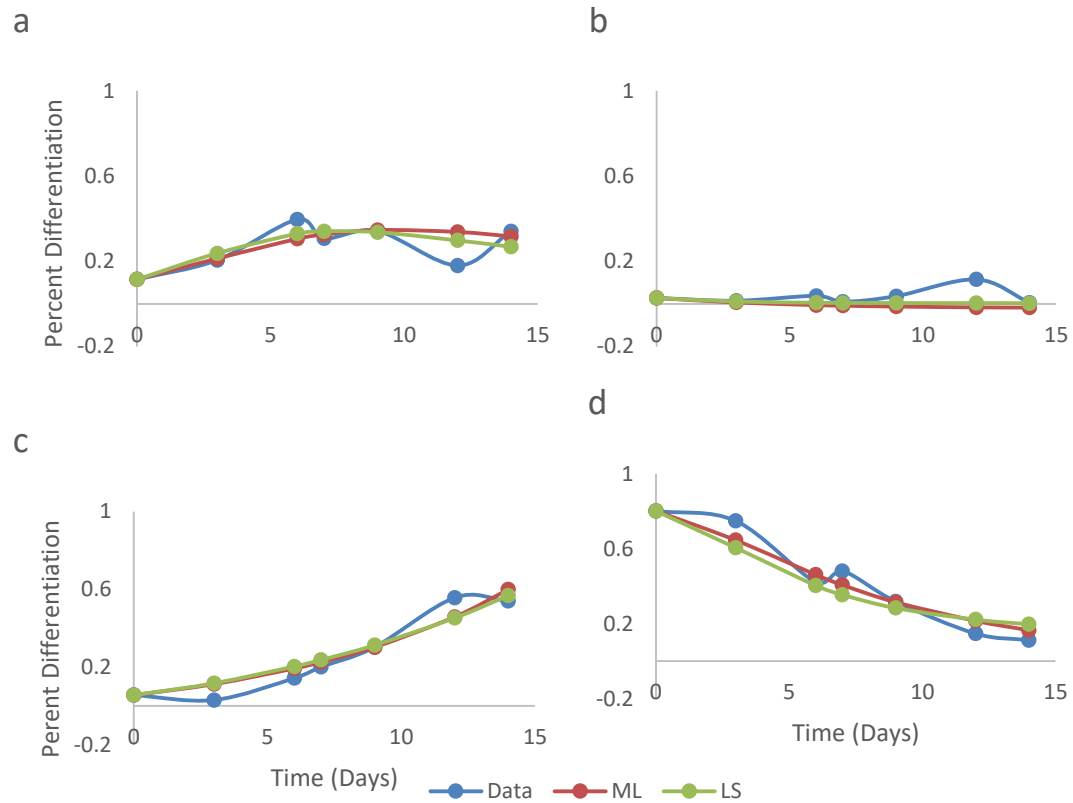
Figure 3.9 Model Simulations of Stem Cell Differentiation in Osteogenic Media.
Maximum likelihood (ML) and least squares (LS) model simulations of
(a) osteogenic differentiation (b) adipogenic differentiation (c) cells
positive for both and (d) neither markers of stem cells for differentiation
of cells cultured in osteogenic media.
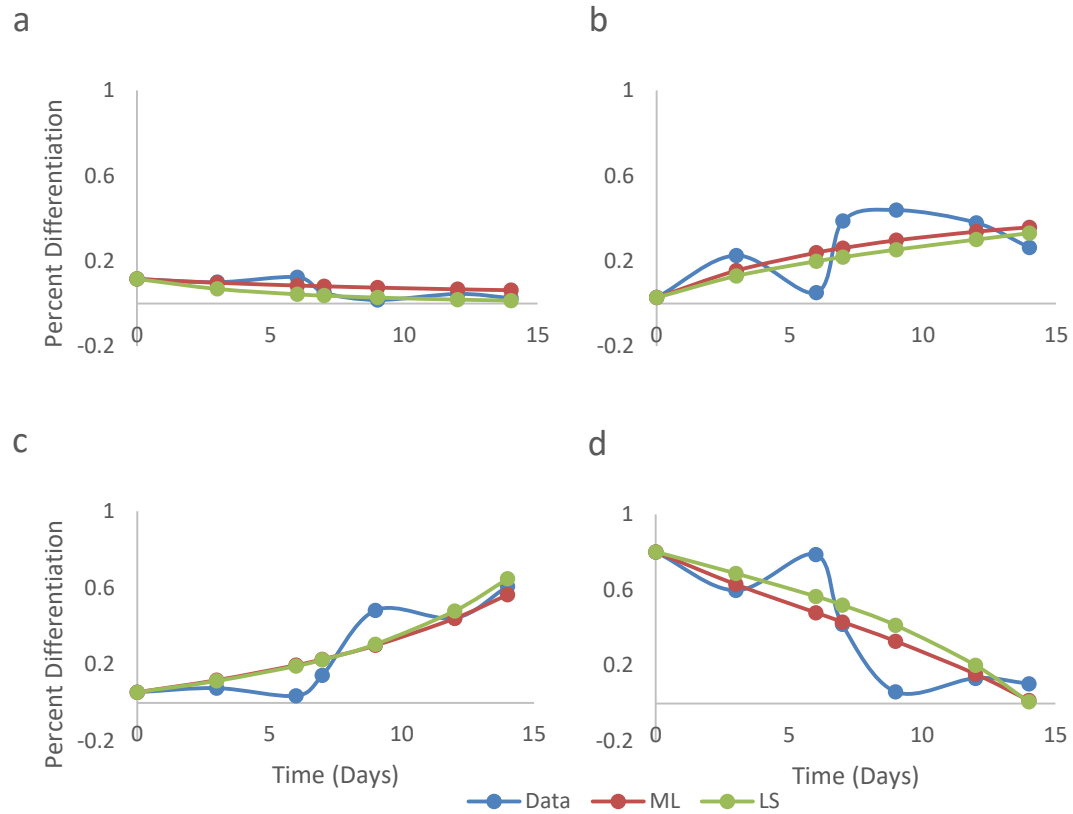
Figure 3.10 Model Simulations of Stem Cell Differentiation in Adipogenic Media.
Maximum likelihood (ML) and least squares (LS) model simulations of
(a) osteogenic differentiation (b) adipogenic differentiation (c) cells
positive for both and (d) neither markers of stem cells for differentiation
of cells cultured in adipogenic media.
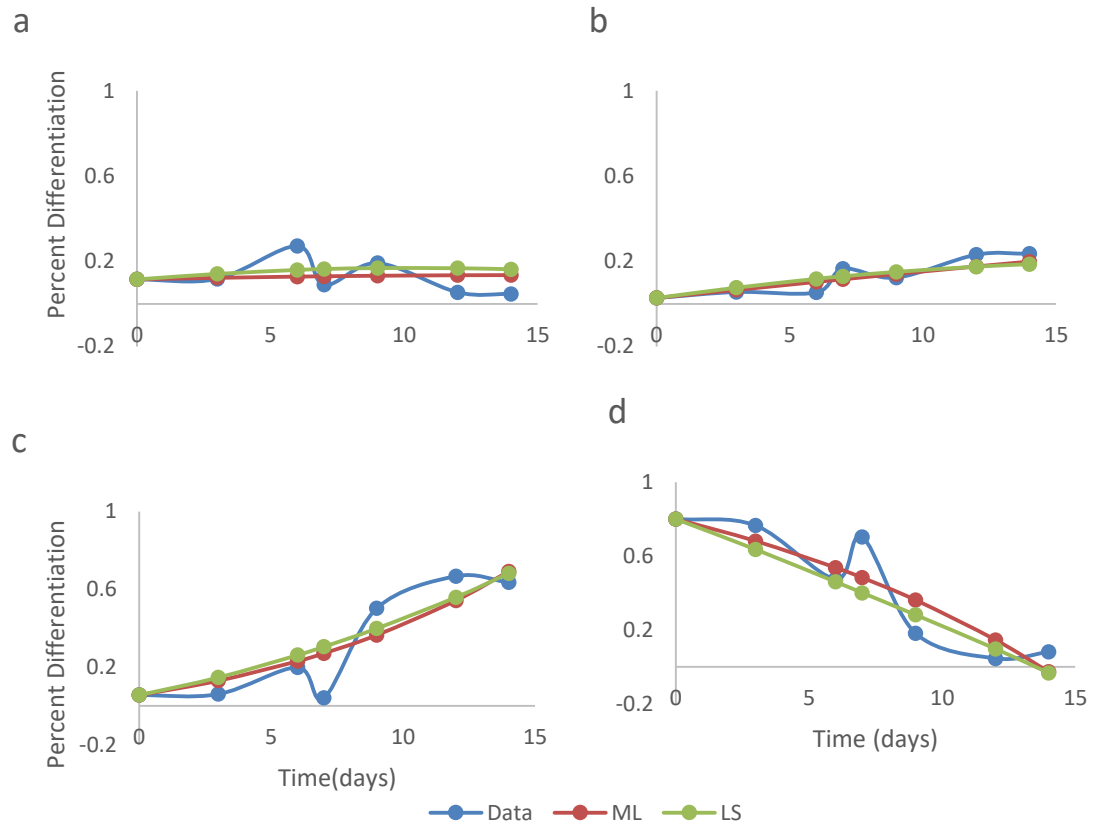
Figure 3.11 Model Simulations of Stem Cell Differentiation in Mixed Media. Maximum likelihood and least squares model simulations of (a) osteogenic differentiation (b) adipogenic differentiation (c) cells positive for both and (d) neither markers of stem cells for differentiation of cells cultured in mixed media.

Using user provided estimates for initial rate constants, the code improves the estimate by either using an iterative method that minimizes the least squares sum, or using a built-in Matlab nonlinear minimizer for the maximum likelihood method (Table 3.2). To determine whether the presence of one differentiation marker hindered the development of a second, the model can estimate rates assuming either that differentiation rates are equal or unequal. The equal differentiation rate hypothesis assumes that development of osteogenic markers in cells positive for neither and cells positive for adipogenic markers are the same ($k_2=k_3$), and similarly that the development of adipogenic markers in cells positive for osteogenic makers and neither makers has the same rate ($k_4=k_5$). Goodness of fit was analyzed using regression analysis (Fig. A4). Model simulations assuming dependent differentiation or unequal values ($k_2 \neq k_3, k_4 \neq k_5$) had smaller residuals than their independent differentiation or equal value ($k_2=k_3, k_4=k_5$) counterparts. Therefore, the equal rates hypothesis is disproven. However, regression analysis showed that neither maximum likelihood nor least squares had consistently smaller residuals, indicating that one model is not superior to the other.

	Media	Model	Rate Assumption	k_1 (1/days)	k_2 (1/days)	k_3 (1/days)	k_4 (1/days)	k_5 (1/days)
Osteo	ML	Unequal	0.579	0.105	0.105	2.212	0.124	0.111
Osteo	LS	Unequal	0.592	0.077	0.077	1.400	0.165	0.149
Osteo	ML	Equal	0.644	0.004	0.004	0.004	0.233	0.233
Osteo	LS	Equal	0.507	0.015	0.015	0.015	0.197	0.197
Adipo	ML	Unequal	0.350	0.034	0.034	0.152	0.103	0.373
Adipo	LS	Unequal	0.652	0.019	0.019	0.146	0.131	0.473
Adipo	ML	Equal	0.078	0.096	0.096	0.096	0.324	0.324
Adipo	LS	Equal	0.702	0.053	0.053	0.053	0.287	0.287
Mixed	ML	Unequal	0.540	0.057	0.057	0.194	0.118	0.176
Mixed	LS	Unequal	0.325	0.019	0.019	0.135	0.131	0.113
Mixed	ML	Equal	0.564	0.038	0.038	0.038	0.333	0.333
Mixed	LS	Equal	0.47	0.035	0.035	0.035	0.320	0.320

Table 3.2   Modeling Estimates of Differentiation Rate Constants. Estimations of rate constants generated by the maximum likelihood method (A,C,E,G,I,K) and the least squares method (B,D,F,H,J,L). Estimations were also exported using equal (k_2=k_3,k_4=k_5) (C,D,G,H,K,L) or unequal rates assumptions (A,B,E,F,I,J).

While the differentiation rates themselves do not clearly explain the differentiation behavior (e.g. k_2, the rate of osteogenic differentiation is not substantially greater in osteogenic media than in adipogenic media), the ratios of rates do describe the trends. By comparing how quickly undifferentiated cells become osteogenic (k_2) to how quickly osteogenic cells become positive for both osteogenic and adipogenic markers (k_5) we can understand osteogenic accumulation. Similarly, adipogenic accumulation is described by comparing the development of an adipogenic marker in undifferentiated cells (k_4) to adipogenic cells developing osteogenic markers (k_3). By comparing these ratios, we can predict which cell phenotype will accumulate in the media. The phenotype with the smaller ratio will be comparatively more transient in the media. k_2/ k_5 is greater than k_4/ k_3 in osteogenic media, indicating adipogenic cells are more transient. Therefore, osteogenesis is greater than adipogenesis in osteogenic media not because the stem cell rate of osteogenic differentiation (k_2) is necessarily greater than the stem cell rate of adipogenesis (k_4), but because adipogenic cells in osteogenic media are more readily positive for both markers. Conversely, osteogenic cells are more transient than adipogenic cells in adipogenic media, and adipogenesis will dominate.

	Media	Model	Rate Assumption	k_2/k_5	k_4/k_3
A	Osteo	ML	Unequal	0.949	0.056
B	Osteo	LS	Unequal	0.518	0.118
C	Adipo	ML	Unequal	0.092	0.679
D	Adipo	LS	Unequal	0.046	0.898
E	Mixed	ML	Unequal	0.325	0.608
F	Mixed	LS	Unequal	0.170	0.967

Table 3.3 Modeling Estimates of Accumulation. k_2/k_5 describes osteogenic accumulation while k_4/k_3 describes adipogenic accumulation.

3.3 Stem Cell Adhesion Site Dynamics as a Function of Biophysical Influences

While biochemical cues are the most common and most popular method of differentiating stem cells, biophysical cues can differentiate stem cells independently of biochemical cues[5,17]. Previous studies show stem cell differentiation as a function of biophysical cues such as substrate stiffness[17], cell spreading[15], and cell shape[15], but lack a proposed method of mechanotransduction. Here we expand our studies to include biophysical influences on stem cell differentiation, by investigating stem cell behavior on substrates of varying stiffness but subject to the same media composition.

In this study, we quantify cell behavior in terms of adhesion site properties. Our hypothesis centers on adhesion sites and outside-in signaling. Adhesion sites lie at the interface of the cell and the environment and we hypothesize that stiff substrates will allow for maturation of larger adhesions compared to their counterparts on soft substrates and that larger adhesions are able to bear more force for a sustained period of time, which may relate to prolonged activation of adhesion site related kinases[35].

To this end, we designed our substrate to isolate the influences of substrate stiffness from other biophysical cues. First, we conjugate a peptide sequence arginine-glycine-aspartic acid-serine (RGDS) isolated from fibronectin to bulk hydrogels. RGDS was chosen to minimize the extracellular matrix whole protein influence on cells. Additionally, different concentrations of RGDS ligand will recruit different amounts of integrins, leading to biased development of adhesion sites which contain signaling molecules[36]. To eliminate this confounding factor, substrate ligand density

was characterized by using fluorescently-labeled, peptide-conjugated monoacrylate PEG. We determined that the fluorescence intensity of a concentration of 3.5 mM on stiff substrates matched the fluorescence intensity of soft gels soaked in 15 mM monoacrylate PEG solution. (Fig. 3.12)

a
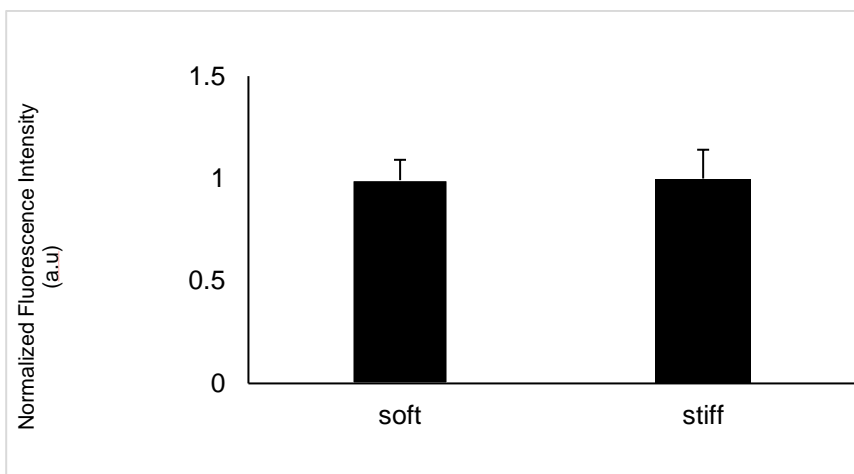
Figure 3.12 Fluorescence Intensity of PEGDA Hydrogels Post Peptide Incorporation.
Normalized fluorescence intensity of 15mM monoacrylate PEG solution
on soft gels (1 kPa) compared to 3.5 mM monoacrylate solution on stiff
gels (101 kPa). (p=0.946)

Compression testing and subsequent analysis at 15% strain revealed the substrate stiffness of bulk PEGDA hydrogels post peptide incorporation to be 1.16±.12 kPa for soft and 101±23 kPa for stiff hydrogels (Fig. 3.13). These stiffness values agree with previously determined values of ~1 kPa substrates inducing adipogenesis and >40kPa substrates inducing osteogenesis[17].
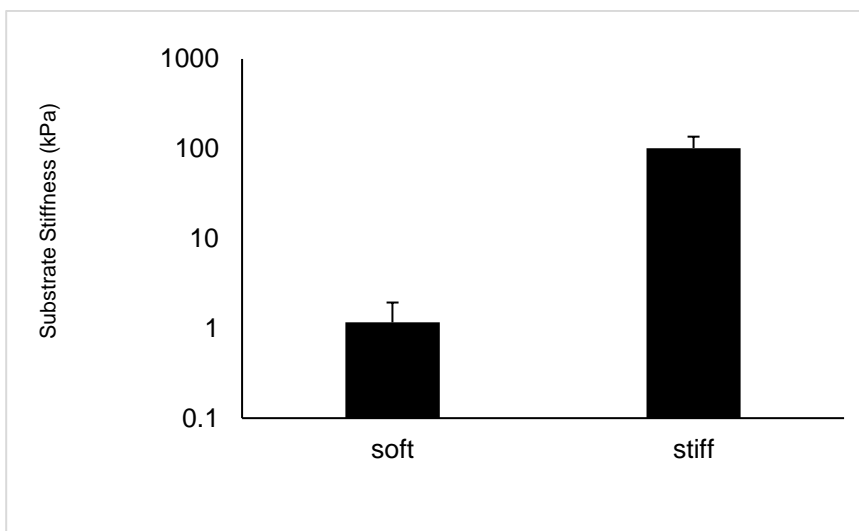
Figure 3.13 Mechanical Characterization of PEGDA Hydrogels. Post peptide incorporation determined by compression testing for soft and stiff bulk hydrogels.

To quantify cell behavior on soft and stiff substrates, we investigate the differences in adhesion sites on cells seeded on different stiffness substrates. Building on the hypothesis that vinculin, a protein localized in adhesions, undergoes a conformational change, we hypothesize that cells on stiff substrates will develop larger more stable adhesions that are capable of prolonged load-bearing, resulting in greater signaling potential of the cryptic binding site. Conversely, we expect cells on soft substrates to be unable to develop large adhesions and will have smaller, more dynamic adhesions.

We visualized cells adhesion sites using GFP-talin, a fluorescently tagged protein that also localizes in adhesions. By imaging over a period of 45 minutes, we observed differences in the adhesion site dynamics of the cells. Subsequently, selectively coloring and overlaying slices, allows us to visualize adhesion dynamics. Each color represents a 7.5 minute interval and adhesions that remain in the same location for the duration of imaging appear to be white (Fig. 3.14, Fig. 3.15). We first compare cells of similar spread area (Fig. 3.14) and then compare a sample of three cells on stiff and three cells on soft substrates (Fig. 3.15),. Images of cells on soft substrates (Fig. 3.14, Fig. 3.15) have fewer white areas than those on stiff substrates, indicating that adhesions in cells on soft substrates are dynamic and less stable. Conversely, images of cells on stiff substrates have substantially more white adhesions, suggesting that they develop larger, more stable adhesions, which may be able to bear not only forces larger in magnitude, but also sustain these forces for longer periods of time. Because of a cryptic MAPK binding site in vinculin[27], we

42

anticipate these differences in adhesion site populations will lead to different temporal profiles of activated MAPK and result in differences in differentiation behavior.

Interestingly, the number of adhesions between cells grown on soft substrates were not statistically significant (p=.27). However, cells on soft substrates formed significantly smaller adhesions than their counterparts on stiff substrates (p=.011) (Table 3.3.1). Power analysis suggests that for our current effect size we will need to perform similar analysis for five more sets of cells to achieve a power of .95.
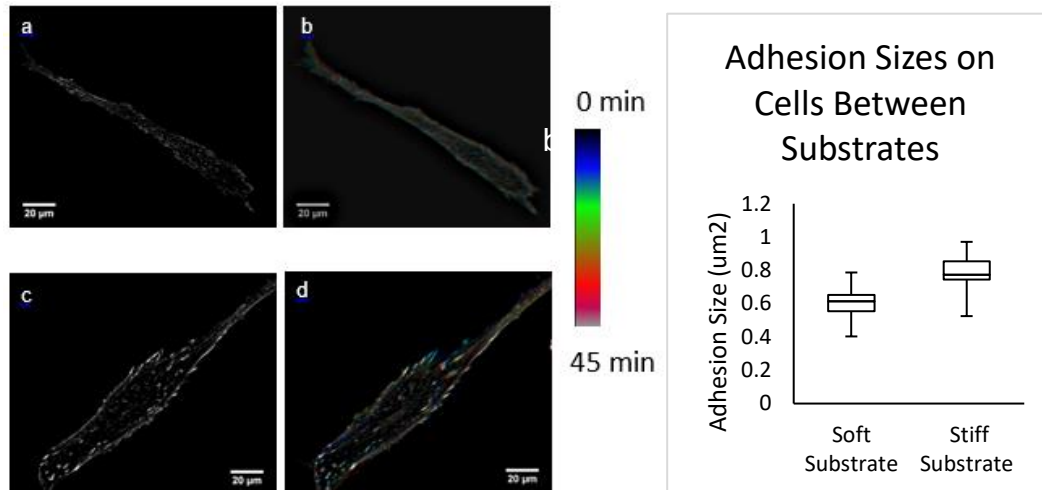
Figure 3.14 Live Cell Imaging on Substrates of Varying Stiffness. Confocal imaging of cells cultured on soft and stiff gels were imaged using GFP-talin. Images were acquired once every 30 seconds for 45 minutes. (a,c) Representative images of cells on (a) soft and (b) stiff hydrogels are shown along with a colored image that depicts a 7.5 minute interval as a different color. Areas shown in white depict adhesion sites that have lasted the entire duration of the 45 minute acquisition period. The graph depicts the differences in adhesion size between these two cells

Soft Substrates

Stiff Substrates

0 min

45 min

Averge Adhesion Size

Adhesion Size (um2)

soft   stiff
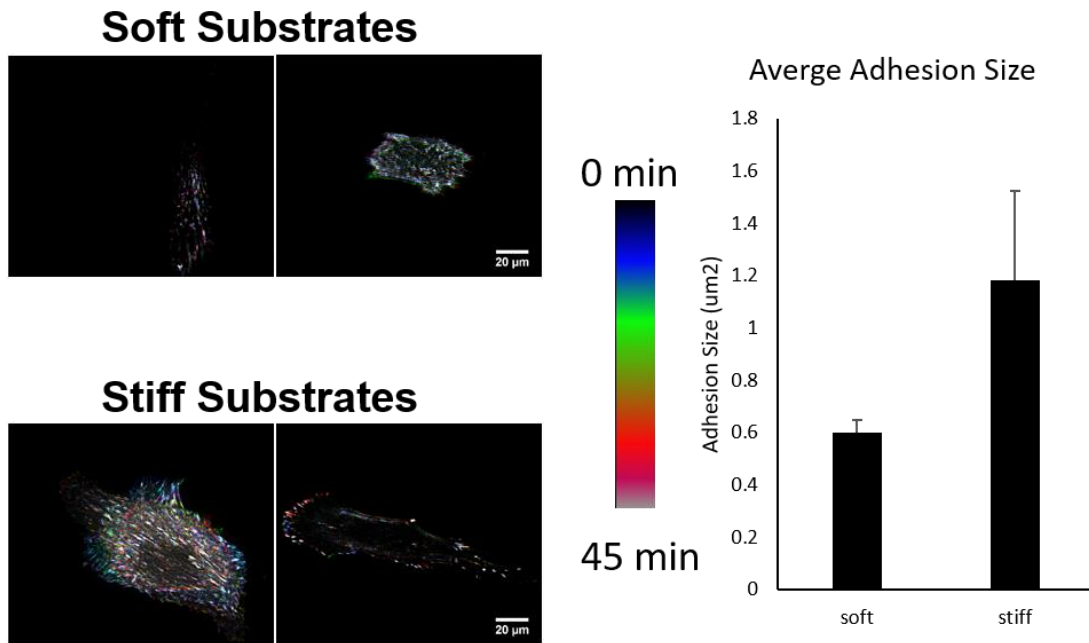
Figure 3.15 Cell adhesion site size between a multiple cells on soft and stiff substrates. Two addition cells on soft and stiff substrates were analyzed using ImageJ for their adhesion sizes. Combining the adhesion size data with the original characteristic cells, we still observe a statistically significant (p<.05) difference between the two populations.

Substrate	A.N. Mean	A.N. Standard Deviation	A.N. P Value	A.S. Mean (um^2)	A.S. Standard Deviation	A.S. P Value
Single Soft	151.6111	35.96712	0.2676	0.547989	0.104006	0.011
Single Stiff	111.9667	50.54855		0.832878	0.068073	
Multiple Soft				1.183796	0.340988	0.03863
Multiple Stiff				0.601113	0.046297	

Table 3.4   Cell adhesion site behavior on soft and stiff substrates. Comparison of adhesion number (A.N) and adhesion size (A.S).

Chapter 4

DISCUSSION

4.1 Stem Cell Differentiation as a Function of Biochemical Influences

Despite noisy data, stem cell differentiation as a function of media revealed populations of cells positive for osteogenic, adipogenic, and both in all three media compositions. While all three media compositions favored a cell population positive for both markers, statistically significant differences existed between osteogenic differentiation and adipogenic differentiation in their respective medium at 14 days.

The population of cells co-expressing osteogenic and adipogenic markers are frequently disregarded in the analysis of differentiation studies. However, the population positive for both markers may still perform osteogenic functions unhindered by the development of lipid droplets[37].

Alternatively, this population may exist because the differentiation markers chosen are early markers. This means that our cell populations are not terminally differentiated and may undergo lineage switching as they are not yet fully committed to an adult lineage[38]. Therefore, use of early markers may also explain the behavior of cells expressing multiple differentiation markers. Additionally expression of early markers may be transient and decrease as cells become further committed to a lineage[39] and studies can be improved by using both an early and a late marker for

47

lineage commitment. For osteogenesis, runx2 and osteopontin[38], and conversely pparg and CCAAT/enhancer binding proteins[40] for adipogenesis

Additionally, our data may also be capturing phenomena that is not accounted for by using different media compositions. For instance, we do not account for the increase in cell density and resulting signaling through cell-cell contacts or paracrine and autocrine signaling[41]. Previous studies indicate high cell density induces more adipogenesis while low cell density induces more osteogenesis[41]. In our study, cells are seeded at low density but are confluent in approximately a week. The influences of cell density are not measured separately but may be influencing subpopulations of cells. Switching from growth to differentiation media during low confluence may initially favor osteogenesis and varying the growth period before differentiation may elucidate more behaviors resulting from varying media composition. Other influences that may influence cells but are not accounted for in our controls is the potential priming of cells. Since we use adipose derived cells, they may be more likely to develop lipid droplets[42]. Conversely, because the cells are cultured on tissue culture plastic, a stiff substrate, mechanical signals may prime cells toward osteogenesis. Despite the use of specific growth factors within the media, we are unable to control all of the stimuli delivered to and epigenetics of stem cells.

Our data is one of the first that show a high population of stem cells positive for multiple seemingly contradictory differentiation markers. We reveal a largely neglected population that requires additional exploration to fully understand the

relative and conditional stem cell differentiation behavior and implications for stem cell-based therapies and technology.

4.2   Mathematical Modeling of Stem Cell Differentiation Behavior

Few mathematical models of stem cell differentiation behavior exist. A previous model of differentiation down osteogenic and myogenic lines used a bistable switch model to describe the lineage commitment of stem cells[31].   Here, we test whether a bistable switch is a good model for differentiation using the equal rates hypothesis. Because a population of cells presented both adipogenic and osteogenic markers, a mutually exclusive bistable switch does not capture the stem cell differentiation phenomena. By developing our own mathematical model, simulations revealed that both maximum likelihood and least squares methods are able to describe the data. Between the maximum likelihood and least squares method, there is not one model that consistently describes the data more than accurately than the other. However, our hypothesis that a model based on a series of ordinary differential equations can describe differentiation behavior is proven.

Even though the bistable switch model currently neglects the population expressing both biomarkers, the model could be expanded to include the population expressing both biomarkers by using two switches, an osteogenic switch that determines positive or negative for ostegenesis, and an adipogenic switch that determines positive or negative for adipogenesis. These switches are independent

meaning that whether a cell is osteogenic or not should not influence whether it is adipogenic or not. If differentiation is dictated by these two switches, both rate constants for developing osteogenic markers should be equal and both rate constants for developing adipogenic markers should be equal ($k_2=k_3,k_4=k_5$).

However, using model simulations, we tested and disproved the equal rates hypothesis ($k_2 \neq k_3,k_4 \neq k_5$) indicating that using two switches does not adequately describe differentiation behavior. Further, this suggests that the development of a differentiation marker is dependent on whether the cell is a stem cell, or already positive for a different marker.

Additionally, we show that the ratio of rates describes the differentiation behavior in different media. We expect that the predicted differentiation rate of osteogenic cells in osteogenic media to be higher than the predicted rate of adipogenic cells in osteogenic media. However, the modeling predictions are not congruent with expectations, but are congruent with the data. Since, osteogenesis is statistically significant compared to adipogenesis in osteogenic media we needed to investigate further to see if our model describes the behavior in a different way. By examining the kinetics of cells becoming positive for a single differentiation marker and their subsequent development of a second differentiation marker, we can reveal some of the behavior of cells. By dividing the rate of stem cells becoming positive for osteogenic markers by the rate of osteogenic cells becoming positive for both, and conversely stem cells becoming positive for adipogenic markers by the rate of adipogenic cells becoming positive for both, we can predict which population is more transient.

Because all of these ratios are less than one, we expect the development of a second differentiation marker to dominate compared to stem cells becoming positive for a single differentiation marker. Further, the values for differentiation markers are higher in their respective medium, which implies that while cells will go toward a phenotype expressing both differentiation markers. Therefore, the development of a second differentiation marker is less transient for a given population, osteogenic or adipogenic, in its respective media.

One aspect of the model that we may not be able to decouple is the differences in upregulation of the adipogenic and osteogenic markers. Alkaline phosphatase is an early marker of osteogenesis while lipid droplet formation is suggested to be slightly later in the adipogenic pathway. We may not be able to separate this phenomena from our data in these models, but in the future, we may be able to choose other or additional differentiation markers to help quantify the osteogenic- or adipogenic potential of cells.

While our model can be further developed to more accurately describe factors of stem cell behavior, we have developed a preliminary way to quantify differentiation in terms of rate constants. Our model can be applied in the future to differentiation behavior of stem cells under other stimuli and has the potential to serve as a tool to compare stem cell behavior between different conditions. Our model begins to fill the need of a standard to compare stem cell differentiation across different experiments investigating biochemical and biophysical influences to optimize a synthetic stem cell niche for efficient stem cell differentiation.

4.3 Stem Cell Adhesion Site Dynamics as a Function of Biophysical Influences

Lastly, we characterized a suitable PEGDA hydrogel platform to continue this work to investigate biophysical influences on stem cell differentiation rates. We present optimized parameters for stiff, bone-like and soft, fat-like hydrogels with the same surface peptide concentration that are capable of supporting cell growth.

Previous studies have shown differentiation as a function of substrate stiffness[17,43] and other biophysical influences[6,41] but frequently do not offer a suggested mechanism for mechanotransduction. Here, we focus on the adhesion sites as they lie at the interface of cells and their environment and while we do not directly measure stem cell differentiation in these studies, we can hypothesize that the adhesion population and adhesion dynamics may play a role in the differentiation process.

Outside of containing kinases such as focal adhesion kinase and SRC[44,45], with known influences downstream signaling cascades, it is hypothesized that vinculin, a force bearing protein localized in adhesions, contains a cryptic MAPK binding site[35]. Adhesions that are larger and more stable may be able to reveal this cryptic binding site for prolonged periods of time while smaller adhesions may only reveal the cryptic binding site for transient periods. Therefore, the differences in adhesion size and dynamics may result in changes in the temporal activation of MAPK. As MAPK increases osteogenic lineage commitment[46,47], our data begins to connect the hypothesized cryptic MAPK binding site with existing literature showing osteogenic

differentiation on stiff- and adipogenic differentiation on soft substrates[17], using live

cell behaviors.

Additionally, because adhesion sites on soft substrates are not as large, we

expect them to be more easily disassembled and have a shorter lifetime than their

larger counterparts on stiff substrates[48]. This likely has an effect on signaling as

proteins behave differently during recruitment and disassembly of adhesion sites[49].

Previous investigations of the contributions of adhesion sites focus on the total

magnitude of force generated by adhesions where larger adhesions are able to generate

larger forces[50,51]. However, we highlight the possibility of a temporal component of

signaling from adhesion sites, an area that has largely been neglected and requires

additional study.

While we have yet to unravel all of the components of adhesion sites that

influence stem cell differentiation, we have developed a live cell imaging method that

has the ability to begin to reveal the intricacies of the role of adhesion sites in

mechanotransduction. Our adhesion analysis highlights the largely unexplored factor

of adhesion behavior and dynamics and stem cell differentiation.

From an alternative approach, the actin cytoskeleton is connected to adhesion

sites through actin binding proteins such as vinculin and talin[52] and also the cell

nucleus[53]. This implies a potential mechanotransduction pathway for tension generated

in adhesions to be transmitted through the cytoskeleton and directly influence the

nucleus. Specifically, large adhesions recruit actin and act as anchors for contractile

stress fibers[54]. A subset of interior stress fibers are connected to nucleus through a

conglomeration of proteins known as the linker of nucleoskeleton and cytoskeleton complex[55]. From there the stress fibers form a perinuclear actin cap which move the nucleus but also interact with inner nuclear membrane proteins[55]. Therefore, the larger, more stable adhesions seen in cells on stiff substrates likely increase direct signaling to the nucleus through the perinuclear actin cap.

Further, we optimized parameters for live cell imaging and presented a method of visualizing the influences of substrate stiffness on adhesion site dynamics which may play a role in cell differentiation due to cryptic binding sites. In the future we hope to also derive simulated k values of differentiation on these substrate for comparison to our soluble growth factor data.

Chapter 5

FUTURE DIRECTIONS

5.1   Stem Cell Differentiation as a Function of Biochemical Influences

Our data shows statistically significant osteogenesis and adipogenesis, but is still subject to population heterogeneity despite being cultured from the same original population. We capture the behavior using mathematical models, and are able to describe stem cell differentiation in terms of differentiation rate constants. Our model now has the potential to compare differentiation under the influence of different biochemical and biophysical stimuli and isolate the most efficient stimuli or combination of stimuli to differentiate cells. However, we have not experimentally tested other differentiation condition.

We have only investigated the biochemical media influence, and would like to design other experiments to further test our model. In the future, we can explore the biochemical influences of cell-cell interactions and cell-matrix interactions. Cell-cell interactions can be studied using micropatterns to dictate the number of neighboring cells. Cell-matrix interactions can be investigated by acrylating different peptide sequences that recruit distinct combinations of integrins. Alternatively, the use of collagen hydrogels or PEG-fibrinogen hydrogels would allow for the comparison of whole protein effects to those of peptides. Further, by using the same live-cell imaging technique described above, we can compare the adhesion site behavior across cells on substrates presenting different peptide sequences or proteins.

Additionally, real time fluorescent reporters such as molecular beacons, quantum dots, or nanoflares can be used to observe the same population of live cells for the two week duration.

5.2 Mathematical Modeling of Stem Cell Differentiation Behavior

While our model is able to accurately fit the data and predict a rate constant, the model is relatively simple. Our equations currently only contain terms that rely on one single population of cells and may not account for all of the interactions that occur during differentiation. Cell interaction terms can be included in the future to capture to cell-cell signaling and influences of cell density on cell differentiation.

5.3 Stem Cell Adhesion Site Dynamics as a Function of Biophysical Influences

First, we were unable to include differentiation data for the imaged cells and would want to pair the adhesion site dynamics with differentiation behavior. Additionally, more analysis can be done to quantify adhesion site dynamics by using deconvolution and particle tracking software.

Live cell imaging in the future could also include fluorescent genetic reporters to more accurately represent the temporal nature of gene expression, eliminate variability derived from studying different sub-populations rather than observing the same sub-population over time, and potentially reveal the interplay of adhesion dynamics, adhesion-localized proteins with cryptic binding sites, and gene expression.

Additionally, we can create micropatterend PEGDA hydrogels to investigate other biophysical influences such as cell shape, spreading, and tension. Traditional photolithography would suffice to create micropatterned PEGDA hydrogels suitable for investigations of cell shape. Lastly, by using image-guided laser-scanning lithography techniques developed in the Slater lab, fiducial markers with an implied zero state can be incorporated into PEGDA hydrogels to quantify cell tension and the resulting effects on stem cell differentiation. These two methods may even be used simultaneously to begin to decouple biophysical influences on cell fate.

REFERENCES

1. Cipriani P, Carubbi F, Liakouli V, et al. Stem cells in autoimmune diseases: Implications for pathogenesis and future trends in therapy. *Autoimmun Rev*. 2013;12(7):709-716. doi:10.1016/j.autrev.2012.10.004.

2. Wang JH-C, Thampatty BP. Mechanobiology of adult and stem cells. *Int Rev Cell Mol Biol*. 2008;271(8):301-346. doi:10.1016/S1937-6448(08)01207-0.

3. Jung M-R, Shim I-K, Kim E-S, et al. Controlled release of cell-permeable gene complex from poly(L-lactide) scaffold for enhanced stem cell tissue engineering. *J Control Release*. 2011;152(2):294-302. doi:10.1016/j.jconrel.2011.03.002.

4. Kilian K a, Bugarija B, Lahn BT, Mrksich M. Geometric cues for directing the differentiation of mesenchymal stem cells. *Proc Natl Acad Sci U S A*. 2010;107(11):4872-4877. doi:10.1073/pnas.0903269107.

5. Kilian K a, Bugarija B, Lahn BT, Mrksich M. Geometric cues for directing the differentiation of mesenchymal stem cells. *Proc Natl Acad Sci U S A*. 2010;107(11):4872-4877. doi:10.1073/pnas.0903269107.

6. Gao L, McBeath R, Chen CS. Stem cell shape regulates a chondrogenic versus myogenic fate through Rac1 and N-cadherin. *Stem Cells*. 2010;28(3):564-572. doi:10.1002/stem.308.

7.   Shakhbazau a V, Petyovka N V, Kosmacheva SM, Potapnev MP. Neurogenic
        induction of human mesenchymal stem cells in fibrin 3D matrix. *Bull Exp Biol
        Med*. 2011;150(4):547-550. http://www.ncbi.nlm.nih.gov/pubmed/22268061.

8.   Oughlis S, Lessim S, Changotade S, et al. The osteogenic differentiation
        improvement of human mesenchymal stem cells on titanium grafted with
        polyNaSS bioactive polymer. *J Biomed Mater Res A*. 2013;101(2):582-589.
        doi:10.1002/jbm.a.34336.

9.   Wyles CC, Houdek MT, Crespo-Diaz RJ, et al. Adipose-derived Mesenchymal
        Stem Cells Are Phenotypically Superior for Regeneration in the Setting of
        Osteonecrosis of the Femoral Head. *Clin Orthop Relat Res*. 2015;473(10):3080-
        3090. doi:10.1007/s11999-015-4385-8.

10.   Bovenberg MSS, Degeling MH, Tannous BA. Advances in stem cell therapy
        against gliomas. *Trends Mol Med*. 2013;19(5):281-291.
        doi:10.1016/j.molmed.2013.03.001.

11.   Fujiwara H, Ferreira M, Donati G, et al. The Basement Membrane of Hair
        Follicle Stem Cells Is a Muscle Cell Niche. *Cell*. 2011;144(4):577-589.
        doi:10.1016/j.cell.2011.01.014.

12.   Antebi B, Pelled G, Gazit D. Stem Cell Therapy for Osteoporosis. 2014:41-47.
        doi:10.1007/s11914-013-0184-x.

13. van der Meer AD, van den Berg A. Organs-on-chips: breaking the in vitro impasse. *Integr Biol (Camb)*. 2012;4(5):461-470. doi:10.1039/c2ib00176d.

14. Lanzoni G, Oikawa T, Wang Y, et al. Concise review: clinical programs of stem cell therapies for liver and pancreas. *Stem Cells*. 2013;31(10):2047-2060. doi:10.1002/stem.1457.

15. McBeath R, Pirone DM, Nelson CM, Bhadriraju K, Chen CS. Cell shape, cytoskeletal tension, and RhoA regulate stem cell lineage commitment. *Dev Cell*. 2004;6(4):483-495. http://www.ncbi.nlm.nih.gov/pubmed/15068789.

16. Ellis SJ, Tanentzapf G. Integrin-mediated adhesion and stem-cell-niche interactions. *Cell Tissue Res*. 2010;339(1):121-130. doi:10.1007/s00441-009-0828-4.

17. Engler AJ, Sen S, Sweeney HL, Discher DE. Matrix elasticity directs stem cell lineage specification. *Cell*. 2006;126(4):677-689. doi:10.1016/j.cell.2006.06.044.

18. Lv H, Li L, Sun M, et al. Mechanism of regulation of stem cell differentiation by matrix stiffness. *Stem Cell Res Ther*. 2015;6:103. doi:10.1186/s13287-015-0083-4.

19. Trappmann B, Gautrot JE, Connelly JT, et al. Extracellular-matrix tethering regulates stem-cell fate. *Nat Mater*. 2012;11(7):642-649.

doi:10.1038/nmat3339.

20.   Discher DE, Janmey P, Wang Y-L. Tissue cells feel and respond to the stiffness
       of their substrate. *Science*. 2005;310(5751):1139-1143.
       doi:10.1126/science.1116995.

21.   Buxboim A, Rajagopal K, Brown AEX, Discher DE. How deeply cells feel:
       methods for thin gels. *J Phys Condens Matter*. 2010;22(19):194116.
       doi:10.1088/0953-8984/22/19/194116.

22.   Théry M. Micropatterning as a tool to decipher cell morphogenesis and
       functions. *J Cell Sci*. 2010;123(Pt 24):4201-4213. doi:10.1242/jcs.075150.

23.   Danhier F. RGD-Based Strategies To Target Alpha (v) Beta (3) Integrin in
       Cancer Therapy and Diagnosis. 2012;(v). doi:10.1021/mp3002733.

24.   Maggio N Di, Martella E, Frismantiene A, Resink TJ. Extracellular matrix and
       α 5 β 1 integrin signaling control the maintenance of bone formation capacity
       by human adipose-derived stromal cells. *Nat Publ Gr*. 2017;(February):1-12.
       doi:10.1038/srep44398.

25.   Dupont S. Role of YAP / TAZ in cell-matrix adhesion-mediated signalling and
       mechanotransduction. *Exp Cell Res*. 2016;343(1):42-53.
       doi:10.1016/j.yexcr.2015.10.034.

26.   Hao J, Zhang Y, Wang Y, et al. Role of extracellular matrix and YAP / TAZ in

cell fate determination. *Cell Signal*. 2014;26(2):186-191.
doi:10.1016/j.cellsig.2013.11.006.

27.   Holle AW, Tang X, Vijayraghavan D, et al. In situ mechanotransduction via vinculin regulates stem cell differentiation. *Stem Cells*. 2013;31(11):2467-2477. doi:10.1002/stem.1490.

28.   Fu M, Wang C, Zhang X, Pestell RG. Signal Transduction Inhibitors in Cellular Function. 284.

29.   Wu J, Tzanakakis ES. Deconstructing stem cell population heterogeneity : Single-cell analysis and modeling approaches. *Biotechnol Adv*. 2013;31(7):1047-1062. doi:10.1016/j.biotechadv.2013.09.001.

30.   Labriola NR, Darling EM. Temporal heterogeneity in single-cell gene expression and mechanical properties during adipogenic differentiation. *J Biomech*. 2015;48(6):1058-1066. doi:10.1016/j.jbiomech.2015.01.033.

31.   Wang L, Walker BL, Iannaccone S, Bhatt D, Kennedy PJ, Tse WT. Bistable switches control memory and plasticity in cellular differentiation. 2009.

32.   Tariq A, Hochfeld WE, Myburgh R, Pepper MS. Adipocyte and adipogenesis. *Eur J Cell Biol*. 2013;92(6-7):229-236. doi:10.1016/j.ejcb.2013.06.001.

33.   Tsai T, Li W. Identification of Bone Marrow-Derived Soluble Factors Regulating Human Mesenchymal Stem Cells for Bone Regeneration. *Stem Cell*

Reports. 2017;8(2):387-400. doi:10.1016/j.stemcr.2017.01.004.

34. Bütikofer L, Stawarczyk B, Roos M, Carlo M. Two regression methods for estimation of a two-parameter Weibull distribution for reliability of dental materials. *Dent Mater*. 2014;31(2):e33-e50. doi:10.1016/j.dental.2014.11.014.

35. Holle AW, Tang X, Vijayraghavan D, et al. In situ mechanotransduction via vinculin regulates stem cell differentiation. *Stem Cells*. 2013;31(11):2467-2477. doi:10.1002/stem.1490.

36. Harris GM, Shazly T, Jabbarzadeh E. Deciphering the combinatorial roles of geometric, mechanical, and adhesion cues in regulation of cell spreading. *PLoS One*. 2013;8(11):e81113. doi:10.1371/journal.pone.0081113.

37. Ponce ML, Koelling S, Kluever A, Heinemann DEH, Miosge N, Wulf G. Coexpression of Osteogenic and Adipogenic Differentiation Markers in Selected Subpopulations of Primary Human Mesenchymal Progenitor Cells. 2008;1355:1342-1355. doi:10.1002/jcb.21711.

38. Lee J, Abdeen A a, Kilian K a. Rewiring mesenchymal stem cell lineage specification by switching the biophysical microenvironment. *Sci Rep*. 2014;4:5188. doi:10.1038/srep05188.

39. Julia C. Chen, Mardonn Chua, Raymond B. Bellon and CRJ. Epigenetic changes during mechanically induced osteogenic lineage commitment. 2015.

40.   Ntambi JM, Kim Y. Adipocyte Differentiation and Gene Expression.
        2000:3122-3126.

41.   McBeath R, Pirone DM, Nelson CM, Bhadriraju K, Chen CS. Cell Shape,
        Cytoskeletal Tension, and RhoA Regulate Stem Cell Lineage Commitment.
        Dev Cell. 2004;6(4):483-495. doi:10.1016/S1534-5807(04)00075-9.

42.   Rath SN, Nooeaid P, Arkudas A, et al. Adipose- and bone marrow-derived
        mesenchymal stem cells display different osteogenic differentiation patterns in
        3D bioactive glass-based scaffolds. 2016;(December 2013). doi:10.1002/term.

43.   Mullen C a, Haugh MG, Schaffler MB, Majeska RJ, McNamara LM. Osteocyte
        differentiation is regulated by extracellular matrix stiffness and intercellular
        separation. *J Mech Behav Biomed Mater*. 2013;28:183-194.
        doi:10.1016/j.jmbbm.2013.06.013.

44.   Slack JK, Adams RB, Rovin JD, Bissonette E a, Stoker CE, Parsons JT.
        Alterations in the focal adhesion kinase/Src signal transduction pathway
        correlate with increased migratory capacity of prostate carcinoma cells.
        Oncogene. 2001;20(10):1152-1163. doi:10.1038/sj.onc.1204208.

45.   Zhao X, Guan J-L. Focal adhesion kinase and its signaling pathways in cell
        migration and angiogenesis. *Adv Drug Deliv Rev*. 2011;63(8):610-615.
        doi:10.1016/j.addr.2010.11.001.

46.   Kim HK, Park KS, Lee JS, et al. Cellular Biochemistry. 2012;1841(September 2011):1833-1841. doi:10.1002/jcb.24052.

47.   Jaiswal D, Brown JL. Nanofiber diameter-dependent MAPK activity in osteoblasts. *J Biomed Mater Res A*. 2012;100(11):2921-2928. doi:10.1002/jbm.a.34234.

48.   Suidan T. Adhesion Dynamics on the Line: The Mass Aggregation Process. 2000;(1):893-903.

49.   Grashoff C, Hoffman BD, Brenner MD, et al. Measuring mechanical tension across vinculin reveals regulation of focal adhesion dynamics. *Nature*. 2010;466(7303):263-266. doi:10.1038/nature09198.

50.   Plotnikov S V, Pasapera AM, Sabass B, Waterman CM. Force Fluctuations within Focal Adhesions Mediate ECM-Rigidity Sensing to Guide Directed Cell Migration. *Cell*. 2012;151(7):1513-1527. doi:10.1016/j.cell.2012.11.034.

51.   Bellas E, Chen CS. Forms, forces, and stem cell fate. *Curr Opin Cell Biol*. 2014;31:92-97. doi:10.1016/j.ceb.2014.09.006.

52.   Ciobanasu C, Faivre B, Clainche C Le. Integrating actin dynamics , mechanotransduction and integrin activation : The multiple functions of actin binding proteins in focal adhesions. *Eur J Cell Biol*. 2013;92(10-11):339-348. doi:10.1016/j.ejcb.2013.10.009.

53.   Khatau SB, Bloom RJ, Bajpai S, et al. The distinct roles of the nucleus and

       nucleus-cytoskeleton connections in three-dimensional cell migration. 2012.

       doi:10.1038/srep00488.

54.   Goffin JM, Pittet P, Csucs G, Lussi JW, Meister J-J, Hinz B. Focal adhesion

       size controls tension-dependent recruitment of alpha-smooth muscle actin to

       stress fibers. *J Cell Biol*. 2006;172(2):259-268. doi:10.1083/jcb.200506179.

55.   Burridge K, Guilluy C. Focal adhesions , stress fi bers and mechanical tension.

       Exp Cell Res. 2016;343(1):14-20. doi:10.1016/j.yexcr.2015.10.029.

.

SUPPLEMENTAL INFORMATION
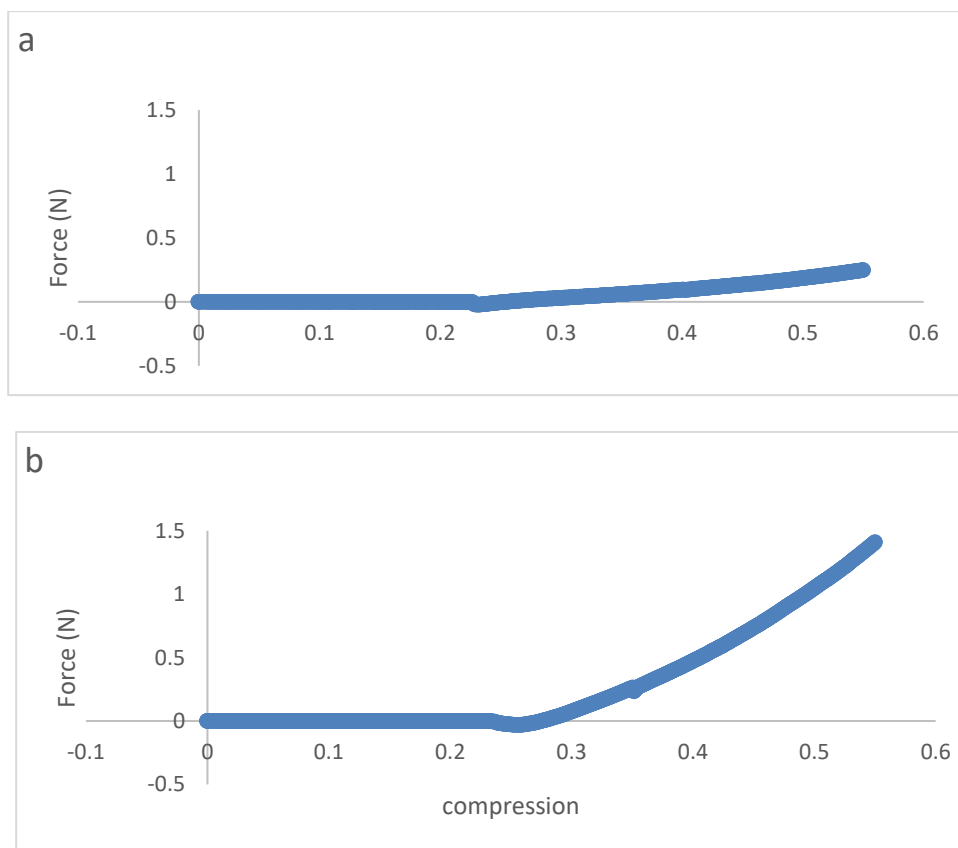
Figure A1   Representative Instron Compression Data of Soft and Stiff Substrates.
Instron compression data for (a) soft and (b) stiff PEGDA hydrogels.
Negative region indicates the attraction of the water in the hydrogel after
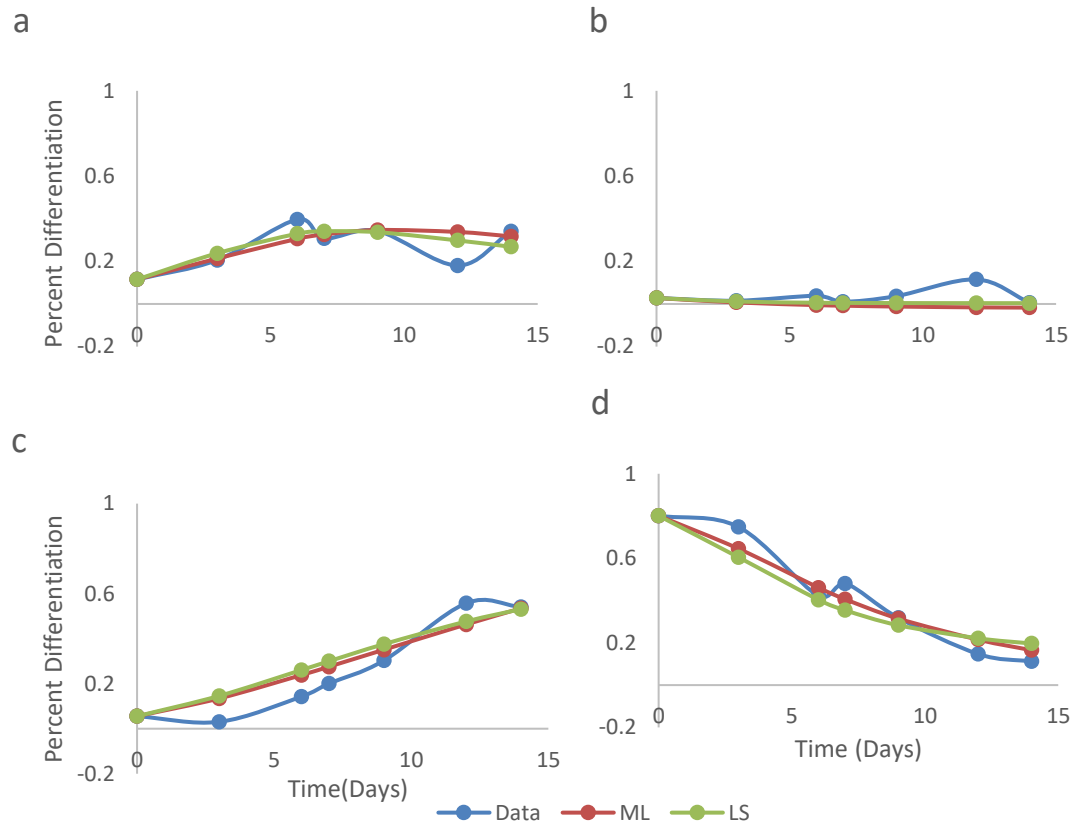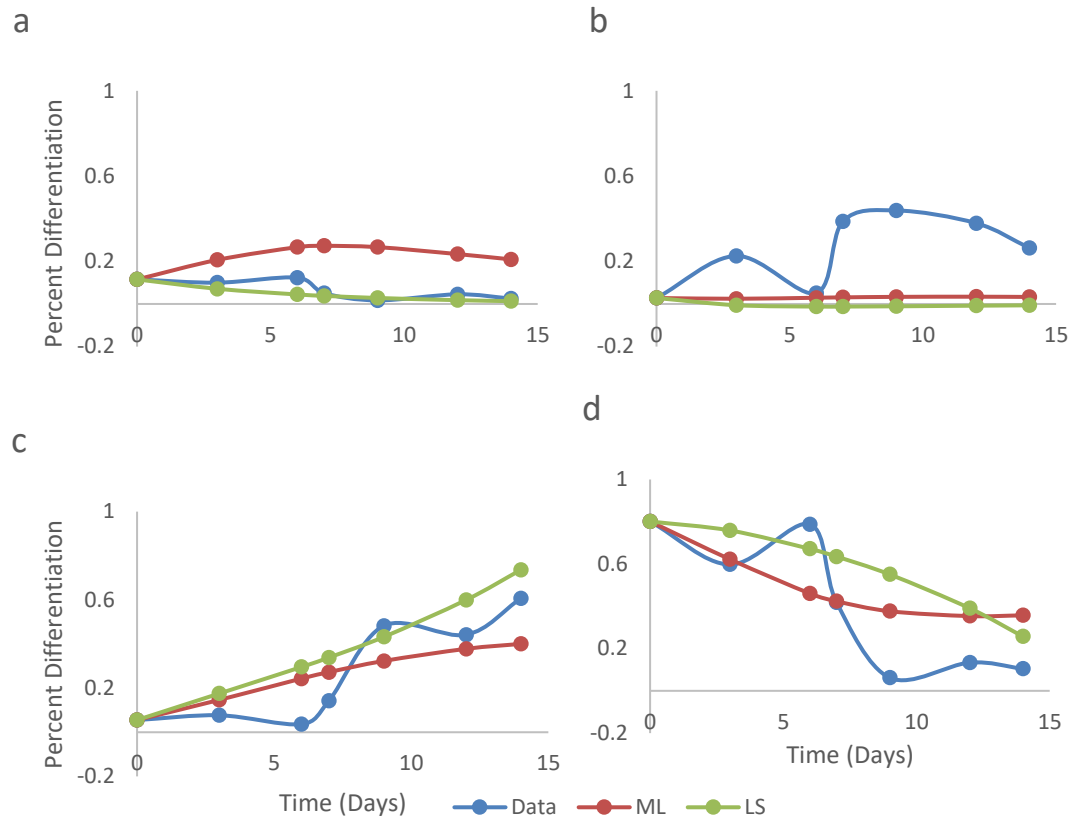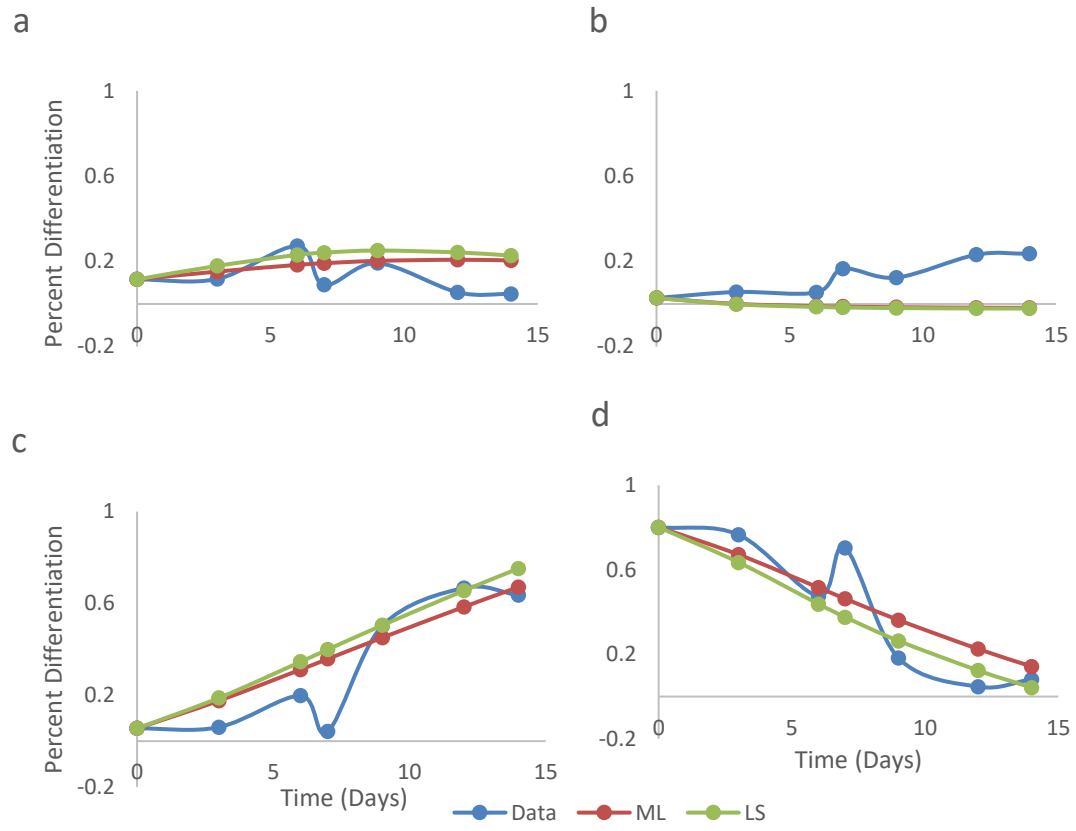contact, before hydrogel compression.

Figure A2   Model Simulation of Stem Cell Differentiation in Osteogenic Media
Assuming Equal K Values. Maximum likelihood (ML) and least squares
(LS) model simulations of (a) osteogenic differentiation (b) adipogenic
differentiation (c) cells positive for both and (d) neither markers of stem
cells for differentiation of cells cultured in osteogenic media with the
equal rates hypothesis ($k_2=k_3, k_4=k_5$).

Figure A3   Model Simulation g of Stem Cell Differentiation in Adipogenic Media
Assuming Equal K Values Maximum likelihood (ML) and least squares
(LS) model simulations of (a) osteogenic differentiation (b) adipogenic
differentiation (c) cells positive for both and (d) neither markers of stem
cells for differentiation of cells cultured in adipogenic media with the
equal rates hypothesis ($k_2=k_3, k_4=k_5$).

Figure A4   Model Simulation of Stem Cell Differentiation in Mixed Media
Assuming Equal K Values. Maximum likelihood (ML) and least squares
(LS) model simulations of (a) osteogenic differentiation (b) adipogenic
differentiation (c) cells positive for both and (d) neither markers of stem
cells for differentiation of cells cultured in mixed media with the equal
rates hypothesis ($k_2=k_3, k_4=k_5$).

Media	Model	Assumption	Osteogenic	Adipogenic	Both	Neither
Osteo	ML	E	0.034036	0.022424	0.036822	0.025093
Osteo	LS	E	0.025726	0.014529	0.049061	0.050918
Osteo	ML	U	0.027423893	0.008073	0.022986	0.020486
Osteo	LS	U	0.028017147	0.01106	0.024112	0.021472
Adipo	ML	E	0.212685	0.50413	0.136593	0.319498
Adipo	LS	E	0.008257	0.641909	0.15923	0.414702
Adipo	ML	U	0.007611502	0.087269	0.069737	0.175667
Adipo	LS	U	0.008606299	0.105049	0.066369	0.205266
Mixed	ML	E	0.067392	0.184215	0.137167	0.135813
Mixed	LS	E	0.099143	0.190854	0.179614	0.139879
Mixed	ML	U	0.039855	0.009582	0.096022	0.113278
Mixed	LS	U	0.045238	0.011945	0.105254	0.133601

Table A1   Least Squares Regression Analysis for Goodness of Fit of Model
Simulations. Statistical analysis on the goodness of fit of model
simulations dependent on media type, model type, and equal
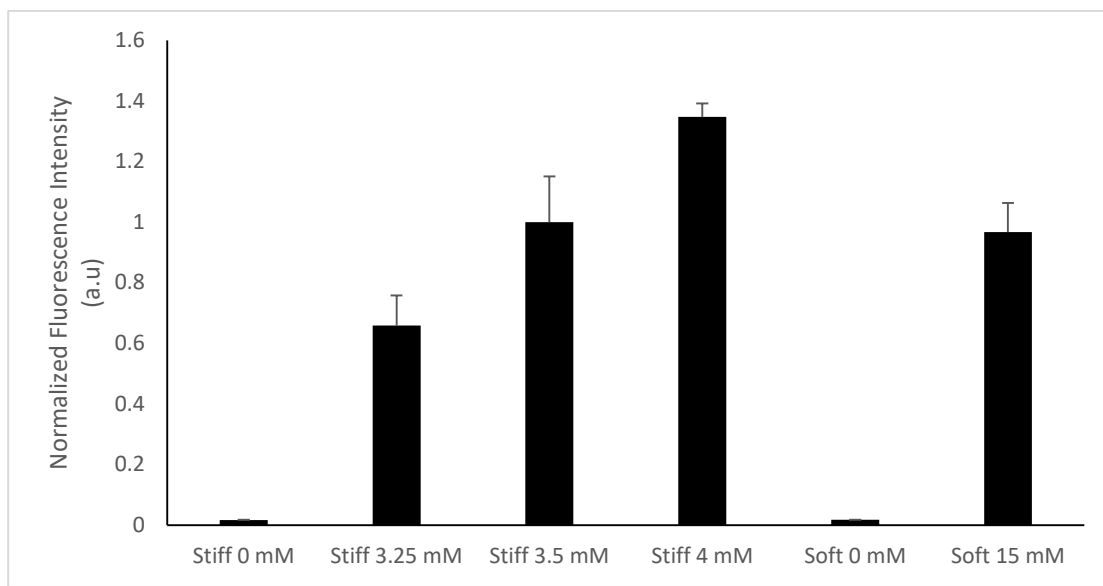($k_2=k_3,k_4=k_5$) or unequal ($k_2{\neq}k_3,k_4{\neq}k_5$) assumptions.

Figure A5   Monoacrylate Peptide Intensity with Control. Identification of a match for 15 mM monoacrylate peptide on soft hydrogels indicating no fluorescence intensity on blank 0 mM PEGDA hydrogels and varying intensity with varying monoacrylate concentration on stiff gels.